Searching for Synergy: FAK Inhibition in Metastatic Breast Cancer Treatment

The Thesis Presented to

The Faculty of Graduate and Post-Doctoral Studies

Of

The University of Ottawa

By Brianna Conway

In partial fulfillment of the requirements for

Master's Degree of Science in Biochemistry with a Specialization in Human and Molecular Genetics

BMI Graduate Program

University of Ottawa

Thesis Advisor

Dr. Christina Addison

Abstract

Breast cancer is the most common cancer among Canadian women and 14-20% will develop lethal metastases within 5 years. A potential novel therapeutic target is Focal Adhesion Kinase (FAK), a cytoplasmic tyrosine kinase. FAK's expression is inversely correlated with survival and is known to regulate cell migration, proliferation and invasion. While tyrosine kinase inhibitors are historically ineffective as single agents, they are commonly used as part of combination therapies.

Therefore, given its central role in tumor cell biology and cell signaling, we hypothesized that inhibiting FAK in combination with pharmacological agents commonly used to treat metastatic breast cancer patients will result in enhanced anti-tumor activity.

We combined a commercial FAK inhibitor (PF-562271) with a range of chemotherapeutic agents commonly used to treat metastatic breast cancer and searched for synergistic partners. Only DNA topoisomerase inhibitors showed potential to synergistically reduce cell viability when paired with low doses of the FAK inhibitor.

However, the combination does not induce an increase in cell death or apoptosis. It was then discovered that both agents in isolation and in combination produce increased levels of ROS, a toxic metabolite. This, along with other more preliminary data, provides clues for a novel proposed mechanism of action for this interaction.

Acknowledgements

I would like to thank Dr. Christina L Addison for affording me the opportunity to train and perform my studies under her supervision, in addition to her help in editing this manuscript. I would also like to thank my thesis advisory committee members Dr. Jim Dimitroulakos and Dr. Luc Sabourin for their guidance and critiques.

I would also like to thank all the past and present members of the Addison lab, in no particular order: Grant, Jane, Steve, Katie, Sara, Victoria, Joseph, Scott, Caroline, Zeinab and Viya, and all my other coworkers with whom I have had the immense pleasure of working with these past few years. Special thanks to Grant for his invaluable insight during the more challenging periods of my project.

Thank you to my parents, Lorne and Shauna Conway, who instilled in me a sense of independence, wonder and ambition for many years. Thank you to all of my friends – SD, GH, AR, AR, HS, JS, LS and CT - for making me laugh and allowing me to find my sense of self among you. A thank you to Master Aqua, for finding me in the dark and teaching me that there is always a way. Lastly to Christopher Guo, thank you for your love, patience, support, and for giving me the confidence to be brave. I am who I am today because of you.

This study was partially supported by research grants provided by the Canadian Breast Cancer Foundation Ontario to Dr. Addison. The research was performed as part of the Cancer Therapeutics Program at the Ottawa Hospital Research Institute.

Table of Contents

List of Abbreviations

2OHEth	**2-hydroxyethidium**
ANOVA	**Analysis of Variance**
BGS	**Bovine Growth Serum**
CI	**Combination index**
DHE	**Dihydroethidium**
DMEM	**Dulbecco's Modified Eagle's Medium**
DMSO	**Dimethyl sulfoxide**
dNTP	**Deoxynucleotide**
DoxR	**Doxorubicin**
DTPA	**Diethylenetriaminepentaacetic acid**
DTT	**Dithiothreitol**
ECM	**Extracellular matrix**
EGFR	**Epidermal Growth Factor Receptor**
Eth	**Ethidium**
Etop	**Etoposide**
FAK	**Focal Adhesion Kinase**
FAT	**Focal Adhesion Targeting**
FBS	**Fetal Bovine Serum**
FERM	**Four-point-one, Ezrin, Radixin, Moesin**
HPLC	**High-performance Liquid Chromatography**
IDC	**Invasive ductal carcinoma**
MTT	**3-(4,5-Dimethylthiazol-2-yl)-2,5-Diphenyltetrazolium Bromide**

MW	**Molecular weight**
NAC	**N-acetyl-L-cysteine**
PF-271	**PF-562271, a competitive FAK inhibitor**
PI	**Propidium iodide**
PVDF	**Polyvinylidene Difluoride**
PYK2	**Proline-rich tyrosine kinase-2**
RIPA	**Radioimmunoprecipitation assay**
ROS	**Reactive Oxygen Species**
RPMI-1640	**Roswell Park Memorial Institute (*RPMI*) 1640**
SDS-PAGE	**Sodium Dodecyl Sulfate Polyacrylamide Gel Electrophoresis**
SOD	**Superoxide Dismutase**
TBST	**Tris buffered saline with Tween**
TCA Cycle	**Tricarboxylic Acid Cycle**
TKI	**Tyrosine Kinase Inhibitor**
Topo	**Topotecan**

List of Figures

List of Tables

Chapter 1: Introduction

1.1 Metastatic Breast Cancer

Breast cancer is the most prevalent cancer among Canadian women. It accounts for more than a quarter (25.8%) of all new female cancer diagnoses in 2016, representing approximately 25 600 women in Canada alone (1). The risk of receiving a breast cancer diagnosis varies depending on a variety of factors, including age, genetics, hormone levels, activity levels, and environmental factors among many others (1). However, the fact remains that, over a given woman's lifetime, she has approximately 12.5% or, 1 in 8, chance of being diagnosed with, and a 1 in 31 chance of dying from, breast cancer (2). This makes breast cancer the second deadliest cancer in terms of incidence for Canadian women, falling only behind lung bronchus cancer (1).

Unfortunately, breast cancer also represents 13% of all cancer-related deaths in women, and carries an overall 5-year mortality rate of 22% (2)(3). This means that annually, breast cancer can be attributed to nearly 5 000 lost lives a year in Canada alone (1).

Encouragingly, according to the SEER Cancer Statistics Review, 5-year overall combined survival for all breast cancer cases has been on a steady increase over the past few decades rising from 75.2% in 1975, 84.6% in 1990 to approximately 89.7% as of 2013 (2). However, while reassuring, this dramatic improvement masks significant variations in 5-year overall survival based on the stage of the cancer at the time of diagnosis and cancer subtype.

Breast cancer exists in many different subtypes. The major distinction lies between non-invasive, or *in situ*, and invasive breast cancer. Non-invasive breast cancers typically remain within the confines of the milk duct or lobule in which they do not invade into the surrounding tissue. Invasive breast cancers, on the other hand, do invade the surrounding tissue (4). Invasive breast cancers account for most

breast cancer diagnoses and are significantly more dangerous. Invasive breast cancer can be further subdivided into a variety of subtypes including ductal, lobular, ductal/lobular, mucinous, tubular and medullary, among others depending on their location of origin and histopathological subtype (4)(5). However, by far the most common subtype of breast cancer is invasive ductal carcinoma (IDC) which accounts for approximately 80% of all diagnosed breast cancers (6), which translates into nearly 20 500 IDC diagnoses in Canada women alone each year (1). IDC can be further subdivided based on the protein expression profiles and level of differentiation (or grade) (7)(8). The five major sub classifications include luminal A, luminal B, triple-negative, HER2-enriched and normal-like and their key differentiating characteristics are listed in **(Table 1).**

Staging of cancer is of critical importance for determining the prognosis for a newly diagnosed breast cancer patient. Staging can be roughly categorized into three major stages, primary localized, regional, and metastatic (2). Primary localized cancers, where the cancer remains only in the part of the body where the cancer originated, in this case the breast alone, carry the least risk. Regional cancers have spread to neighbouring tissue, typically lymph nodes in the case of breast cancer, and carry slightly more risk (1) (3) (6). Metastatic cancer, where the cancer has spread to distant tissue, which in the case of breast cancer is most commonly, in descending order of likelihood, bone, liver, lung or brain, by far carries the most risk (2) (12). Metastatic breast cancer, like all metastatic cancers, is incurable, and eventually fatal in nearly all cases. Primary localized and regional breast cancers have relatively high 5-year survival rates (98.8% and 85.2% respectively), and yet the 5-year overall survival for women diagnosed with *de novo* metastatic breast cancer drops to a mere 26.3% (1) (2).

For those women living with metastatic disease, the formation of tumours in distant tissues can cause an increase in cancer-related morbidities. Since breast cancer often metastasizes to the bone, skeletal related events (pathological fractures, spinal cord compressions, hypercalcemia etc.) are not

infrequent and could necessitate additional hospitalization, surgery or radiation (13). It has also been shown that 30.6% of all breast cancer patients, regardless of staging, present with micrometastases, metastatic growths too small to be detected by conventional means, in their bones at the time of diagnosis. (14) While only half of these patients will ever develop a proper symptomatic metastatic relapse, the presence of these micrometastases is still an independent marker of poor prognosis (14).

	Protein Expression Status				Grade	Outcome	Prevalence
	ER	PR	HER2	KI67			
Luminal A	+	+	-	-	Low to Moderate	Good	34%
Luminal B	+	+	-/+	+	Moderate to High	Intermediate to Poor	18%
Triple-Negative (Basal-like)	-	-	-	+	High	Poor	25%
HER2-Enriched	-	-	+	+	Moderate to High	Poor	18%
Normal-Like	+	+`	-	-	Low to High	Intermediate	5%

Table 1: Summary of Molecular Subtypes of IDC.

Summary of the five major molecular subtypes of IDC along with their grade, outcome and prevalence. ER= Estrogen Receptor, PR= Progesterone Receptor, HER2= Human Epidermal Growth Factor Receptor-2. Derived from (9), (10), and (11).

1.2 Current Treatments for Metastatic Breast Cancer

The many treatment regimens for women with metastatic breast cancer are varied and depend largely on the location, subtype and severity of the metastases. These include, among many other forms of treatment, a vast array of chemotherapeutic agents with a variety of mechanisms of action.

Microtubule synthesis inhibitors, like docetaxel and vinorelbine, prevent the formation of the tubulin fibre complexes required for mitosis to occur. DNA crosslinking agents like cisplatin and cyclophosphamide, form covalent bonds within the structure of the DNA strand and produce double stranded breaks in the DNA sequence which prevent cells from completing S-Phase, leading to cell arrest and death. Antimetabolite compounds, such as 5-fluorouracil, function through a similar mechanism, but introduce toxic nucleotides which inhibit DNA replication. 5-fluorouracil, for example, directly inhibits thymidylate synthase, a critical DNA replication enzyme, and incorporates itself into DNA and RNA further preventing replication (15). Topoisomerase inhibitors, such as doxorubicin and topotecan, function by inhibiting topoisomerases, DNA unwinding proteins critical during replication preventing its completion, leading to irreparable DNA strand breaks (either single or double stranded breaks depending on the agent) and subsequently cell death (16)(17). Depending on the molecular subtype of the breast cancer, hormone blocking agents are also given in conjunction with chemotherapeutic treatment. These include estrogen blocking compounds such as anastrazole and tamoxifen which target estrogen synthesis and estrogen receptors on the surface of the cell respectively (16) (17) (18). This is in addition to more recent monoclonal antibody treatments such as trastuzumab which targets and inhibits HER2 receptors directly by preventing ligand binding (16) (17) (19). There are even a few metastatic-specific treatments for breast cancer however, though they depend largely on the location of the metastasis. For example, compounds that inhibit osteolysis, such as the bisphosphonates zoledronate and pamidronate, as well as more modern RANKL inhibitors such as denosumab, are

commonly used in the treatment of bone metastases to prevent osteoclast activity and thereby prevent tumour-induced bone degradation (20).

Unfortunately, while routine treatment using chemotherapy and hormone blockers has been proven to prolong overall survival in metastatic patients with certain receptor- positive subtypes (such as Luminal A, Luminal B and HER2-enriched), the gains have been modest at best, and do not affect those with triple negative phenotypes (21) (22). Further still, while there is significant evidence suggesting the addition of osteolysis inhibitor compounds can decrease the morbidity associated with skeletal related events, they have little to no impact on overall survival figures for women with metastatic disease (23)(24). While the estimates vary with the cancer subtype, the median survivability post-diagnosis for all metastatic breast cancer patients was 20 months in 1993, 21 months in 1998, 25 months in 2003 and still remains a mere 28 months as of 2014 (25) (26).

Thus, it is imperative that research be performed to discover novel therapeutic targets and therefore novel treatment regimens in the metastatic setting in order to promote survival for these women. One such recent target was epidermal growth factor receptor (EGFR), which is overexpressed in 20-25% of all breast cancers, and is associated with poor clinical outcomes (27) (28). However, the results of various clinical trials have shown little or no ability for an EGFR blocker to work as either a single agent or as a chemosensitizer (27). While disappointing, it could be possible that, in the presence of an EGFR blocker, another compensatory downstream pathway would be upregulated. One such downstream effector of EGFR signalling is focal adhesion kinase, whose downregulation improves the efficacy of EGFR inhibitors *in vivo* and in non-small cell lung cancer (29) (30). This effect is primarily due to the fact that focal adhesion kinase crosstalks with EGFR, and is downstream of integrin signalling pathways (30). Even more encouragingly, even outside the EGFR context, focal adhesion kinase is a potential therapeutic target in its own right, and is the primary subject of this study.

1.3 Focal Adhesion Kinase (FAK)

Focal adhesion kinase (FAK) is a 125 kDa protein that is expressed by most adherent cells in the body (31). FAK is a non-receptor cytoplasmic tyrosine kinase typically associated with the intracellular machinery of the focal adhesion complex (32).

FAK is comprised of several important domains, including among others, a focal adhesion targeting (FAT) domain, the kinase domain, the activation loop and the four-point-one, exrin, radixin moesin (FERM) domain (33). These structural domains influence FAK's kinase and kinase independent activity as described in **(Figure 1).** In its deactivated state, the FERM domain is closely associated with and auto-inhibits the kinase domain **(Figure 1, Panel 1)** (32) (34)**.**

Amongst the primary activators of FAK are integrins, transmembrane proteins that give cells their ligand binding specificity (35). Upon binding to their extracellular matrix (ECM) ligands, a conformational change occurs in the integrin complex between the α and β integrin subunits, forming the complete heterodimeric integrin. This conformational shift leads to the recruitment of intracellular adhesion -associated proteins such as paxillin and talin **(Figure 1, Panel 2)** (34). The recruitment of these proteins forms the initial components of the intracellular focal adhesion complex. The focal adhesion complex refers to the cytoplasmic recruitment of a vast array of proteins following integrin binding to ECM (36). These proteins range from signalling proteins such as FAK and talin to structural proteins such as actin and myosin (36). It has a wide variety of functions from cytoskeletal modification to the promotion of survival pathways to proliferation. However, for the sake of simplicity in this study, we will be focussing primarily on a few select signal transduction pathways of molecules paxillin, talin and FAK.

The FAT domain of FAK localizes to talin in this newly formed complex. This localization instigates a structural shift in the FAK FERM domain which partially detaches itself from the kinase domain, revealing a critical tyrosine residue on the kinase domain, Y397 **(Figure 1, Panel 3)** (37). This

Y397 residue then auto-phosphorylates and prompts yet another conformational change within the kinase domain, completely detaching it from FERM domain. This detachment reveals the activation loop, which connects the FERM and kinase domains, and had previously been obscured and protected from phosphorylation **(Figure 1, Panel 4)** (34) (37). The phosphorylation of Y397 also produces a high-affinity recruitment site for the SH2 domain of Src, which subsequently binds to FAK **(Figure 1, Panel 5).** The newly recruited Src phosphorylates further residues on the activation loop, including Y576 and Y577. **(Figure 1, Panel 6)** (37). This highly phosphorylated state, in complex with Src, is the fully activated state of FAK.

FAK is expressed by the Ptk2 gene. There is a very similar gene, Ptk2B, which encodes the closely related proline-rich tyrosine kinase-2 (PYK2). PYK2 shares 60% sequence identity with FAK, particularly in its kinase domain. Whereas the phosphorylation of Y397 of FAK creates the SH2 binding site necessary for the recruitment of Src, it is the phosphorylation of Y405 and Y881 of PYK2 that creates a similar SH2 binding site for GRB2 (38) (32) (39). However, there are distinct differences between the two proteins. Among others, as the name implies, FAK typically localizes to focal adhesion complexes, whereas PYK2 has a perinuclear distribution (32). When FAK was knocked down in fibroblasts, increased PYK2 levels were observed to promote cell survival (40). In addition, *in vitro* FAK knockout has been shown to increase RHO GTPase activity (41) and angiogenesis (42) via upstream PYK2 activation. This functionality could inhibit the ability of FAK-targeted therapy. In fact, PYK2 phosphorylation has been proven to increase in the presence of a FAK-selective inhibitor (42). It should be noted then that most FAK-inhibitors used in a clinical setting, including the one used herein, function as dual FAK-PYK2 inhibitors to mitigate this compensatory response to decreased FAK levels by PYK2.

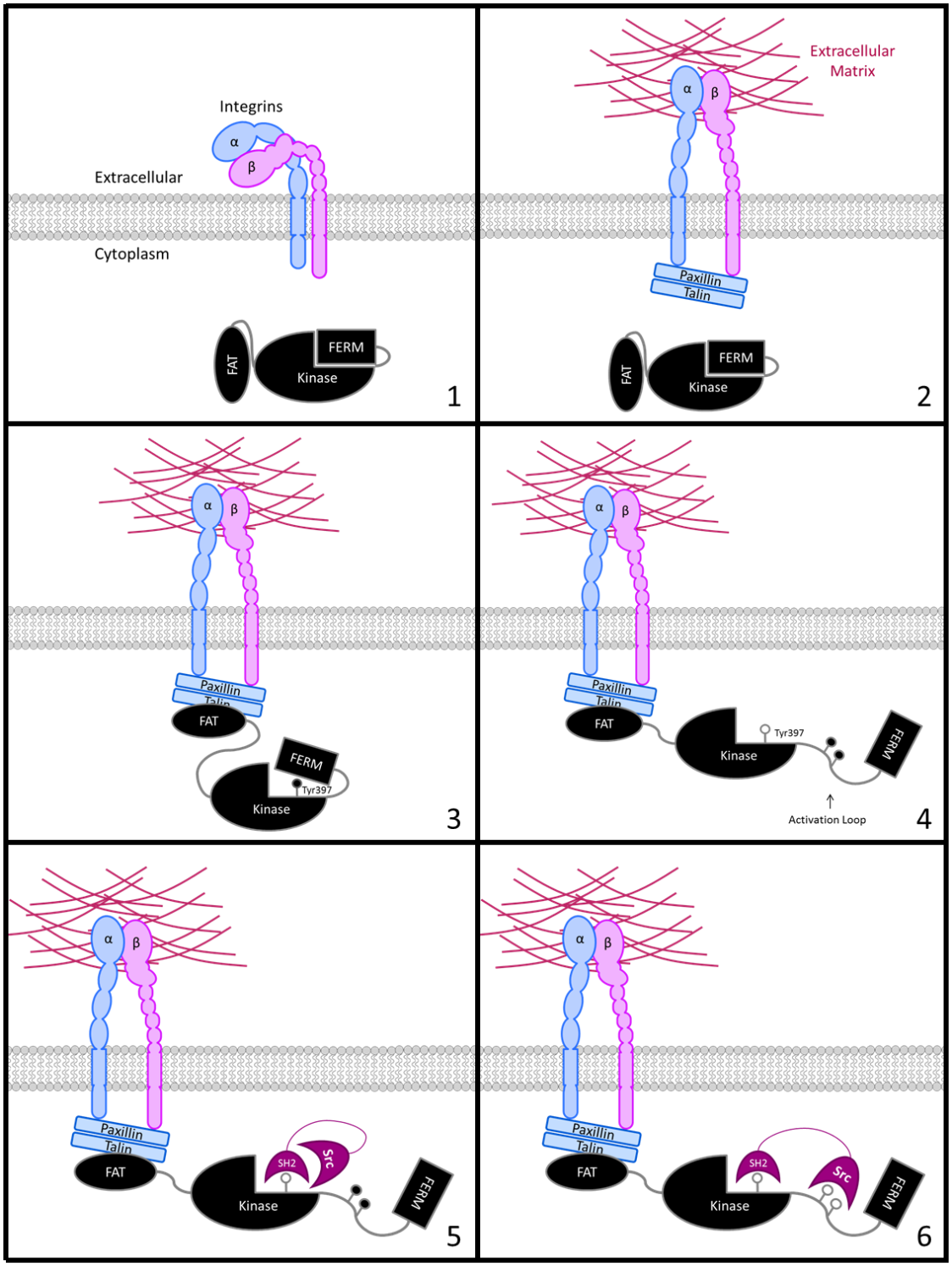

Figure 1: Structure and Function of FAK Overview.

Illustration of how the structure and phosphorylation states of FAK affects the function and binding affinities of its various domains. Derived from (32) (33) (34).

1.4 FAK and Cancer

FAK and especially the activated FAK-Src complex described above, plays a critical role in many cellular processes integral to metastatic cancer behaviour. Three canonical hallmarks of cancer are impacted by FAK: increased proliferation, evasion of cell death and apoptosis, and increasing capacity for invasion and metastasis (43). Many of such pathways are summarized in **(Figure 2)**.

FAK is known to be upstream of biochemical pathways that promote proliferation. Over-expression of FAK resulted in Cyclin D1 upregulation, whereas a mutant FAK which has lost the ability to phosphorylate Y397 leads to a decrease in Cyclin D1 as well as decreased Erk activation (44). In fact, reducing the expression of FAK in micrometastases in mice decreased their rate of growth. This is also true of knocking down integrin β1, an upstream regulator of FAK (45).

FAK is also known to increase cell survival. One of the most studied mechanisms is pY397 FAK's ability to activate the PI3k-Akt pathway. Activated pY397 FAK binds the p85 subunit of PI3K which activates Akt (46). Akt is a potent pro-survival gene, and its activation induces the repression of p53, p73, and caspase-mediated apoptosis (47). FAK's repression of p53 is of particular interest as p53 is a potent pro-apoptotic signalling protein (48). FAK, when translocated into the nucleus, is known to promote the formation of the Mdm-2-p53 complex, which promotes the degradation of p53 via ubiquitination (48). This is particularly important in a cancer context as a decrease in p53 functionality, either through mutation or in this case degradation, is a trait commonly associated with many different cancer subtypes, including breast cancer (49).

Perhaps most studied is FAK's ability to modulate migration and invasion pathways. Activation of FAK is known to be an inhibitor of anoikis (46), where detachment from the ECM results in apoptosis-mediated cell death. This is important for the formation of distant metastases as a cell must first dislodge itself from the primary tumour and survive travel in the bloodstream before establishing itself

in distant tissue (43). FAK is also heavily involved in cell motility pathways. This includes proteins like ARP2/3 and cortactin, which affect actin nucleation and polymerization respectively (50). FAK also binds and activates many members of the RHOGEF family, which controls both actin and microtubule structure formation (32). This is in addition to FAK's namesake influence on proteins associated with the structure and function of the focal adhesion complex, such as talin and paxillin (38). Cell motility and cytoskeletal remodelling is the key to allowing extravasation and invasion; properties critical to the formation and progression of metastatic cancer (43). Critically, the knockdown of FAK has been shown to decrease the rate of metastasis in transgenic mouse models of breast cancer (51).

FAK is also known to crosstalk, via the activated FAK-Src complex, with a variety of growth factor receptors. This crosstalk allows the activation of proliferation and survival signals in a receptor-ligand independent manner. This crosstalk severely compromises the ability of TKIs which target these receptors from being effective (30). One such example is EGFR, as mentioned earlier, which is ineffective as a single agent, but the inclusion of a FAK inhibitor overcomes this resistance, leading to cell death (30).

In all, upregulation and activation of FAK is a key regulator of many processes critical to metastatic growth and proliferation. It would follow then that FAK would be upregulated in metastatic cancer. This has in fact, proven to be the case at both the transcriptomic and protein level in many different cancer subtypes (52) (53). Further, upregulation has also been shown to correlate inversely with overall survival (53). Therefore, FAK would make for a potent target for cancer therapy, especially in a metastatic context.

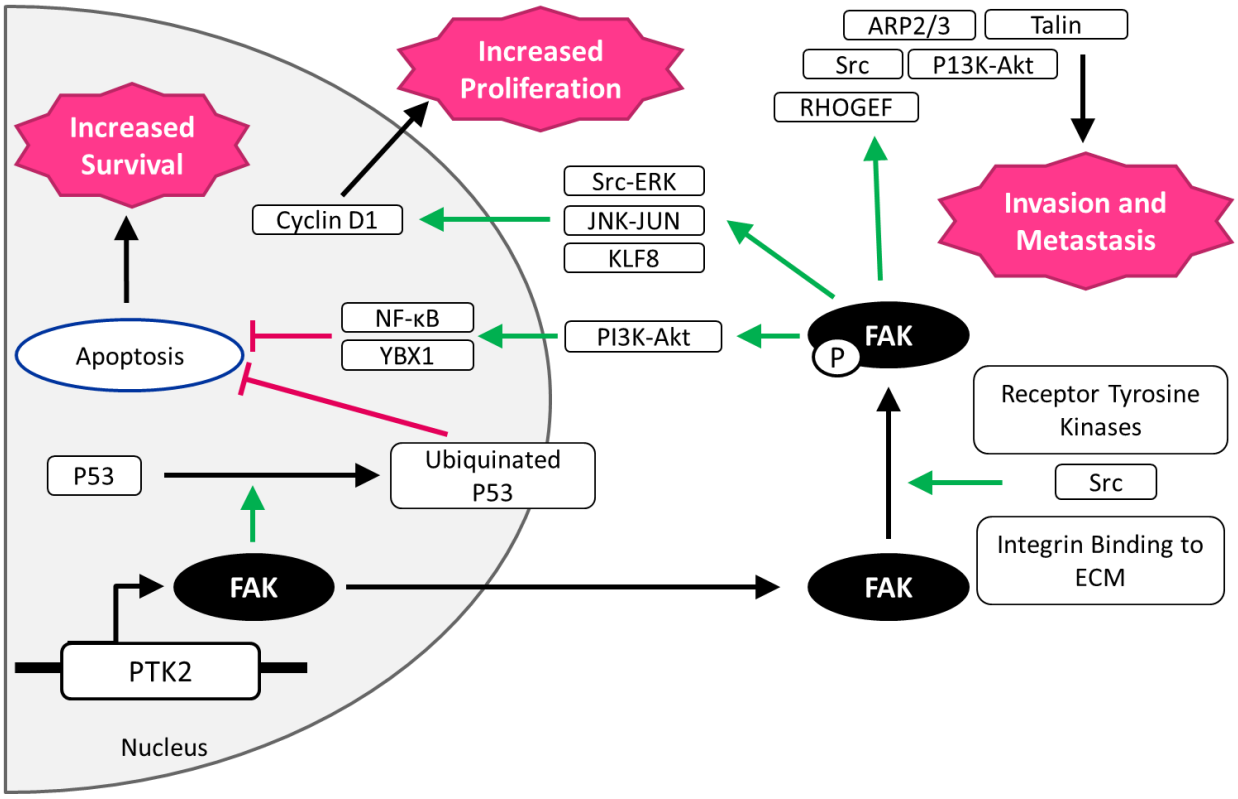

Figure 2: FAK and its Influence in Cancer Overview

Overview of focal adhesion kinase (FAK) in metastatic cancer behavior and development. Green arrows indicate upregulation and red T-bars denote inhibitory regulation. Derived from (34) (54) and (38).

1.5 FAK as a Therapeutic Target in Breast Cancer Treatment

Preclinical trials regarding FAK inhibition in a cancer context have thus far been promising. There have been several studies showing that the inhibition of FAK in preclinical studies of pancreatic and breast cancer reduces metastasis formation, and even prevent bone degradation (55) (56). There is evidence also that FAK inhibition, for both breast and ovarian cancer cells grown in 3D culture, induces cell death (38).

Preliminary Phase I clinical studies have been performed assessing the safety of using a FAK inhibitor, in most cases an ATP-mimetic which prevents the phosphorylation of the critical Y397 residue, and its use in humans has been deemed safe (38) (57). However, despite the promising *in vitro* and *in vivo* studies mentioned earlier, thus far, no FAK inhibitor has yet shown the ability to pass Phase II clinical trials for efficacy as a single agent, despite repeated clinical trials on a variety of tumour types (38).

This outcome should not be surprising however. Historically, tyrosine kinase inhibitors are not typically used as single agent treatments unless the targeted TK is essential for growth (58). There are notable exceptions however. For example, erlotinib is an inhibitor of EGFR, one such TK essential to growth. Erlotinib, has shown promise to prevent proliferation as a single agent in the treatment of non-small cell lung cancer (59). Another example would be trastuzumab, as mentioned earlier, which is occasionally used as a single agent to treat HER2 expressing breast cancers (60) (61). Unfortunately however, this efficacy has not been shown for any FAK inhibitors examined thus far.

However, there is extensive use of tyrosine kinase inhibitors as adjuvant therapies (58). Trastuzumab is used commonly in combination with various classical chemotherapies to treat HER2+ breast cancer (19). It should therefore be possible that combining FAK inhibition with classical chemotherapies would result in an improved cytotoxic effect. Recent literature suggests this to be the

case. One such study combined a siRNA knockdown of FAK with docetaxel; a common chemotherapeutic used to treat ovarian cancer, and showed that in the presence of reduced FAK, the cells were more sensitive to the effects of docetaxel (62). Another showed that inhibiting FAK using a small molecule inhibitor improved the response of xenografted mice containing lung and melanoma cells to both doxorubicin and ionizing radiation (63). FAK inhibition has even been shown to improve the efficacy of trastuzumab in HER2-receptor positive breast cancer lines (64).

1.6 Summary

In summary, FAK is a cytoplasmic tyrosine kinase and a key protein regulator of several pathways integral to metastatic behaviour and would therefore make for a promising target for treatment in the context of metastatic breast cancer. While inhibition of FAK is unlikely to prove useful as a single agent chemotherapeutic, there is literature supporting its capacity to function as a synergistic partner to existing chemotherapeutic treatments. With the urgent need for novel therapies for metastatic breast cancer, further exploitation of FAK inhibition in addition to existing therapy regimens could provide a meaningful increase in survival for these women.

1.7 Hypothesis and Objectives

Hypothesis

Given its central role in tumor cell biology and cell signaling, inhibiting FAK in combination with pharmacological agents commonly used to treat metastatic breast cancer patients will result in enhanced anti-tumor activity.

Objectives

1. *Determine the efficacy of a FAK inhibitor in breast cancer cells*
    - 1.1. *Confirm efficacy of chemical inhibitor PF-271 in multiple breast cancer cell lines to impede FAK function.*
    - 1.2. *Investigate PF-271's ability to inhibit cell viability in cultured breast cancer cells.*
2. *Identify potential synergistic partners to combine with the FAK inhibitor to further reduce breast cancer cell viability.*
    - 2.1. *Combine a FAK inhibitor with chemotherapeutic compounds currently used as standard of care in metastatic breast cancer treatment and perform cell viability assays.*
    - 2.2. *Expand study to perform a secondary specialized drug screen focusing on the class of chemotherapeutics which showed the most synergy with FAK inhibitor in the first screen.*
3. *Investigate mechanism of sensitization for effective drug combinations at the protein and transcriptomic level*
    - 3.1. *Determine mechanism of cell viability decrease*
    - 3.2. *Determine if FAK activity is impacted by synergistic partner*
    - 3.3. *Determine what, if any, survival pathways are affected*
    - 3.4. *Determine what, if any, cell stress pathways are affected*

Chapter 2: Materials and Methods

2.1 Breast Cancer Cell Lines & Growth Conditions

All breast cancer lines used herein are invasive ductal carcinoma cell lines as they represent 80% of all diagnosed breast cancers (6). In this study, three of the most popular cultured breast cancer cell lines from ATCC® were used, MCF7 (HTB-22™), T47D (HTB-133™) and MDA-MB-231(HTB-26™) (65). Combined these three cell lines cover a variety of molecular subtypes, listed in **(Table 2)** below, for metastatic invasive ductal carcinoma.

MCF7 cells were grown in Dulbecco's Modified Eagle's Medium (DMEM) + 4.5g/L glucose, 4.0mM L-glutamine and 110mg/L sodium pyruvate (Corning™, Corning, NY). T47D was cultured in Roswell Park Memorial Institute (RPMI) 1640 + 2.05mM L-glutamine (HyClone™, Chicago, IL). Lastly, MDA-MB-231 cells were grown in DMEM + 1g/L glucose, 4.0mM L-glutamine and 110mg/mL sodium pyruvate (Gibco™, Waltham, MA). All cell lines were grown in their respective growth media in 37°C and 5% CO_2, supplemented with 10% 1:1 fetal bovine serum (FBS) (Gibco™, as distributed by Thermo Fisher Scientific, Waltham, MA) : bovine growth serum (BGS) from (HyClone™, as distributed by GE healthcare, Chicago IL) solution.

All cell lines were reseeded at an approximate density of 1:10 twice a week following washing with PBS (Corning™, Corning, NY), incubation with Trypsin-EDTA (0.05% trypsin, 0.53mM EDTA in HBSS, Corning) for 5min at 37°C followed by the addition of an equivalent volume of the appropriate FBS:BGS containing media.

	MCF7	T47D	MDA-MB-231
ER	+	+	-
PR	+	+	-
HER2	-	-	-
KI67 expression	Low	Low	High
P53 status	wt	mut	mut
Molecular Subtype	Luminal A	Luminal A	Triple Negative

Table 2: Summary of Cell Lines Used

Summary of the phenotypic and genotypic differences in the cell lines used in this study. ER= Estrogen Receptor, PR= Progesterone Receptor, HER2= Human Epidermal Growth Factor Receptor-2, wt=wild-type, mut=mutated. Derived from (66) (67) (68) (69).

2.2 Western Blotting

Total protein from a combination of both adherent and floating cells was isolated following lysis using 80µL radioimmunoprecipitation assay (RIPA) buffer (20mM Tris, 5mM EDTA, 150mM NaCl, 1% NP40, 0.5% sodium deoxycholate, 0.1% SDS in ddH_2O) and collected using a cell scraper. Cell lysates were then frozen at -80°C overnight to complete lysis. Cell lysates were then vortexed and centrifuged at 17 000xg in a tabletop centrifuge at 4°C for 5min. Protein-laden supernatants were then collected and quantified by creating a 1mL solution containing 798µL ddH_2O, 200µL Bio-Rad Protein Assay Reagent (Bio-Rad, Hercules, CA) and 2µL of protein sample. Absorbance was recorded at 595nm using a Thermo Scientific Evolution™ 60S UV-visible spectrophotometer (Thermo Fisher Scientific, Burlington, ON) and converted into µg/mL protein concentrations using a standard curve generated from known quantities of protein.

Appropriate protein samples were selected and run with equal amounts of protein per lane on 1.5mm sodium dodecyl sulfate polyacrylamide gel electrophoresis (SDS-PAGE) gels containing a 10% resolving gel below a 5% stacking gel at 120V for approximately one hour. Proteins were then transferred to a 0.45µM pore size Hydrophobic Immobilon™-P polyvinylidene difluoride (PVDF) Transfer Membrane (MilliporeSigma, St. Louis, MS) over 120min at 80V. Membranes were then probed with the appropriate primary and secondary antibodies, listed below, in either 5% (w/v) skim milk powder in Tris buffered saline with Tween (TBST; 10 mM Tris pH 8.0, 150 mM NaCl, 0.05% Tween 20, referred to herein as 5% milk) or 5% BSA in TBST (referred to herein as 5% BSA) . Membranes were then incubated for approximately 90min in appropriate monoclonal primary antibody solution at room temperature followed by three 5min washes in approximately 10mL of TBST. This was followed by a 60min incubation for conjugated secondary antibodies, again at room temperature, followed by five 5min washes with 10mL of TBST. Proteins were then visualized using Bio-Rad Clarity™ ECL blotting substrate (Bio-Rad, Hercules, CA) in a GeneGnome 5 75000 Bio-imaging Chemiluminescence System (Syngene™, Frederick, MD) used according to manufacturer's instructions. For re-probing of blots, membranes were stripped using stripping buffer (1% w/v SDS, 1.7% w/v NaCl, 1.5% Glycine, pH=2) three times for 5min per wash at room temperature, followed by five washes with TBST. The blots were then re-probed with additional antibodies as described above.

The antibodies used herein are as follows: pY397 FAK – monoclonal mouse (Clone 18/FAK (pY397), BD Biosciences™, San Jose, CA) in 5% BSA at 1:1000 dilution; FAK – monoclonal mouse (Clone 77/FAK, BD Biosciences™, San Jose, CA), in 5% milk at 1:1000 dilution; β-actin – monoclonal mouse anti-β-actin antibody (Clone AC-74, MilliporeSigma, St. Louis, MO), in 5% milk at 1:5000 dilution; and Anti-mouse secondary – Horse-radish peroxidase conjugated Mouse IgG (Clone AP124P, MilliporeSigma St. Louis, MO), 5% milk at 1:5000 dilution.

2.3 FAK Inhibitor & Chemotherapeutics

The commercially available FAK/PYK2 inhibitor PF-562-271 (referred to herein as PF-271) (Cayman Chemical, Ann Arbor, MI) was used as a model small molecule FAK inhibitor for this study. All chemotherapeutics used in the panel were acquired as solutions from the Ottawa Hospital Cancer Center Pharmacy and used without modification, with the exception of topotecan which was obtained as a powder from the same source and reconstituted in water.

2.4 Drug Combination Viability Assays & Combination Index Analysis

Cell viability was assessed using two distinct assays, MTT and Trypan Blue.

The MTT method involved plating 5000 cells in each well of a 96 well plate in 75µL of media, and incubating overnight at 37°C. Subsequently, the cells were treated with an additional 75µL of media containing 4x concentrate of each experimental drug, both in isolation and in combination, with DMSO used as a vehicle control and returned to incubator for 48h. A 42µL aliquot of 5mg/mL (3-(4,5-Dimethylthiazol-2-yl)-2,5-Diphenyltetrazolium Bromide) (MTT) was added at 48h post-drug treatment, incubated at 37°C for 3 hours, then exposed to 84µL of lysis buffer (0.01M HCl in 10% SDS). After overnight incubation with both MTT and lysis solution, absorbance at 570nm was recorded using the Multiskan™ Microplate Spectrophotometer (Thermo Fisher Scientific, Burlington, ON). Absorbance readings were then converted to cell viability by normalizing to the absorbance of cells grown under control no drug (Dimethyl sulfoxide, DMSO) conditions. The final results of three biological replicates were then derived from the average of 8 technical replicates per growth condition per biological replicate.

The Trypan Blue method, involved plating 500 000 cells per well in 6-well plates overnight in 2mL of media which were subsequently treated the following day. After 48h post-treatment, the media was aspirated, and each well was washed with 1mL of PBS. A 500µL aliquot of trypsin was then added to

each well, and incubated for 10min at 37°C. After incubation, 1mL of media was added to each well. A 750µL aliquot of each well was then assessed using a trypan blue exclusion assay, and the number of viable cells were counted using a Vi-CELL Cell Viability Analyzer (Beckman Coulter, Pasadena, CA) under default conditions. The cell number was then doubled to accurately reflect the number of cells in a given well. Results of three biological replicates were averaged and plotted with standard error. IC_{50} concentrations, where applicable, were derived using a superimposed exponential trend line model on Microsoft Excel.

Assessments of combination index (CI) were derived using CompuSyn for Drug Combinations and for General Dose-Effect Analysis. The program was originally developed by Ting-Chao Chou (Memorial Sloan-Kettering Cancer Center, New York, NY) and Nick Martin (Massachusetts Institute of Technology, Cambridge, MA). Analysis via CompuSyn reveals if a given combination produces multiplicative results. If the combination index (CI) value for a given arrangement of compounds produces additive results, the CI value will equal (or closely approximate) 1. If a given arrangement produces antagonistic effect, the CI value will be greater than one (up to a theoretical limit of 2), with larger values indicating more significant antagonism. Conversely, if a given arrangement produces synergistic effects, the CI value will be less than 1 (to a theoretical limit of 0). P-values presented for the combination analysis were derived using a Tukey's post-hoc test following a one-way ANOVA.

2.5 mRNA expression measurements via RT-qPCR

RNA samples were extracted using the RNeasy® kit (Qiagen, Toronto, ON) according to the protocol for mammalian cells. Both supernatant and adherent cells were collected and pooled prior to RNA extraction. Cells were then lysed in RLT buffer before extracting and stored at -80°C. EconoSpin® All-In-One Silica Membrane Mini Spin Columns (Epoch Life Sciences, Sugar Land, TX) were used in place

of the RNeasy® mini spin columns contained in the kit, but protocol was followed according to kit instructions otherwise. RNA samples were stored at -80°C.

Quantification of RNA was performed using 2µL of purified RNA, as above, using a Nanodrop 1000® (Thermo Fisher Scientific, Waltham, MA). Up to 1000ng of RNA was combined with up to 10µL of RNase-free water, and then incubated with 1µL each of 50µM Random Hexamers (Invitrogen, Burlington, ON) and 10µM deoxynucleotide (dNTP) mix. Samples were then heated to 65°C for 5min using a GeneAmp® PCR System 9700 thermocycler (ABI, Burlington, ON). The following was then added to each sample, 4µL of 5x Strand buffer, 2µL 0.1M dithiothreitol (DTT), and 1µL RNase OUT™ Recombinant Ribonuclease Inhibitor (Invitrogen, Burlington, ON). Samples were then heated to 37°C for 2min. Subsequently, 1uL of M-MLV Reverse Transcriptase (Invitrogen, Burlington, ON) was added to each sample followed by incubation at 25°C for 10min, 37°C for 50min and 70°C for 15min. RNase Free water was then added to the sample proportionally to the amount of RNA added at the start of the cDNA preparation protocol in order to produce a 100ng/mL final concentration.

qPCR reaction solutions at a final volume of 10µL were created containing 5µL SyBr Green ROX qPCR Mastermix (Qiagen, Toronto, ON), 0.3µL 10µM forward primer, 0.3µL 10µM reverse primer, 1µL diluted cDNA (see above) and 3.4µL RNase-free H_2O. Solutions were plated in the wells of a MicroAmp™ Optical 96-Well Reaction Plate (Applied Biosystems, Foster City, CA) which was then centrifuged at 1000 rpm for 1min. Plates were then run using the Applied Biosystems® 7500 Fast Real-Time PCR System. The following run method was used: Hold at 50°C for 20 sec, followed by a 10min hold at 95°C. This was then followed by 40 cycles of 95°C for 15sec then 60°C for 1min. A continuous melt curve was produced immediately afterwards using the following sequence: 95°C for 15sec, 60°C for 1min, 95°C for 30sec, then 60°C for 15sec. β-actin was used as an endogenous control in order to calculate ΔΔCt values.

Only intron-spanning primers were used. The sequences are as follows:

Bcl2 forward: AGTACCTGAACCGGCACCT; Bcl2 reverse: GCCGTACAGTTCCACAAAGG;

Bcl2-L1 forward: AGCCTTGGATCCAGGAGAA; Bcl2-L1 reverse: AGCGGTTGAAGCGTTCCT;

β-Actin forward: AGAGCTACGAGCTGCCTGAC; and β-Actin reverse: AGCACTGTGTTGGCGTACAG.

2.6 Flow Cytometry

Cells were plated at a concentration of 500 000 cells per well in 6-well plates, allowed to adhere overnight, and then treated the following day. Following treatment, supernatant was collected in a 15mL conical tube. Remaining cells were washed with 1mL PBS (Corning™, Corning, NY) then treated with 0.5mL of trypsin-EDTA (Corning™, Corning, NY) for approximately 5min at 37°C. A 1mL aliquot of appropriate cell growth media (See above) was added following incubation, and the combined 1.5mL cell solution was then transferred to the same conical tube containing the previously collected supernatant. Tubes were then centrifuged at approximately 1000rcf for 5min to pellet the cells. The cell pellet was then twice washed with 2mL PBS and centrifuged at 1000rcf for 5min. Resulting cell pellet was then re-suspended in 0.5mL of -20°C 70% EtOH to permeabilize the cells then stored in solution at 20°C until flow analysis could be performed.

On the day of flow cytometric analysis, 1mL of PBS was added to each sample, and the cells pelleted via centrifugation at 1000rcf for 5min. Cells were then washed in 1mL PBS and pelleted again as before. After removing PBS, cells were then resuspended in 1mL of a solution of 48µg/mL propidium iodide (PI) and 40µg/mL RNase A in PBS. Cells were then incubated in the dark at 4°C for 30min.

After incubation, samples were read on the FL2 channel of a Beckman Coulter FC500 flow cytometer. The percentage of apoptotic cells was calculated by gating cells with less than 2n genomic content using CXP analysis software (Beckman Coulter, Pasadena, CA) using a discriminator value of 45 for forward scatter.

2.7 Detection of Reactive Oxygen Species

Cells were plated at a concentration of 500 000 cells per well in 6-well plates in 2mL of media, allowed to adhere overnight, and then treated with drugs of interest the following day. Following treatment, cells were washed two times in PBS containing 100µM diethylenetriaminepentaacetic acid (DTPA). Cells were then incubated in modified Hank's Buffer (1.3mM $CaCl_2$, 0.8mM $MgSO_4$, 5.4mM KCl, 0.4mM KH_2PO_4, 4.3mM $NaHCO_3$, 137mM NaCl, 0.3mM Na_2HPO_4, 5.6mM glucose, pH7.4) containing 100µM DTPA and 50µM dihydroethidium (DHE) (MilliporeSigma, St. Louis, MS) for 30min at 37˚ C in the dark. All subsequent steps were performed in minimal light conditions as much as possible. Cells were washed two times in PBS containing an additional 100µM DTPA and harvested in acetonitrile. Lysates were then centrifuged at 12000rcf for 10min at 4˚ C. Supernatant was transferred to a fresh tube and vacuum dried using medium setting for approximately 1-2h or until the acetonitrile had been removed.

High performance liquid chromatography (HPLC) analysis following pellet isolation was performed by Dr. Chet E Holterman, of the Dr. Chris Kennedy Lab at the Kidney Research Centre of the Ottawa Hospital Research Institute according to the following protocol, as taken directly from (70) without modification:

"Pellets were resuspended in 20% Methanol, 79.9% ddH2O and 0.1%Trifluoroacetic acid. Briefly, 100µl was injected into the system and separated under a gradient of solutions A (20% methanol with 0.1% trifluoroacetic acid) and B (100% methanol) at a flow rate of 0.5 ml/min. A Zorbax 300SB C18 (Agilent, Santa Clara, CA) with a 5µM internal diameter was used as the column. The gradient started at 0% solution B and increased linearly during the first 10 minutes to 50% solution B. Solutions were then held at this proportion until 20 minutes, at which time a 5 minute wash using 100% solution B was done. The system was then re-equilibrated with 0% solution B from 25 to 35 minutes. DHE (the probe, and internal standard) was monitored by ultraviolet absorption at 245 nm and yielded a peak at

approximately 9.5 mins. Ethidium (representing non-specific reactive oxygen species, ROS) and 2-hydroxyethidium (representing superoxide) were monitored by fluorescence detection with an excitation of 480 nm and an emission of 580 nm and yielded peaks at approximately 12.5 and 12.9 mins respectively."

2.8 Statistical Analyses

Unless otherwise stated, all statistical tests, including two-tailed t-tests, one-way ANOVA and subsequent corrected multiple comparisons tests (including Tukey's and Bonferroni), were performed using a combination of Prism 6.0 (GraphPad, La Jolla, CA), and graphed using Microsoft Excel.

Chapter 3: Results

For the purposes of our study, we used a commercially available FAK inhibitor, and combined it in an *in vitro* setting with commonly used chemotherapeutics often used to treat metastatic breast cancer patients. The inhibitor chosen was a dual PYK2/FAK inhibitor which functions as an ATP mimetic that reversibly binds to the ATP binding pocket in the kinase domain of FAK. This inhibits autophosphorylation at the Y397 residue, and prevents FERM detachment, and the subsequent Src recruitment necessary for full activation of FAK **(Figure 3).** This inhibitor was then investigated as a chemosensitizer for a variety of chemotherapeutics representing a variety of chemotherapeutic drug classes, followed by specialized investigations if a drug-class specific effect is determined.

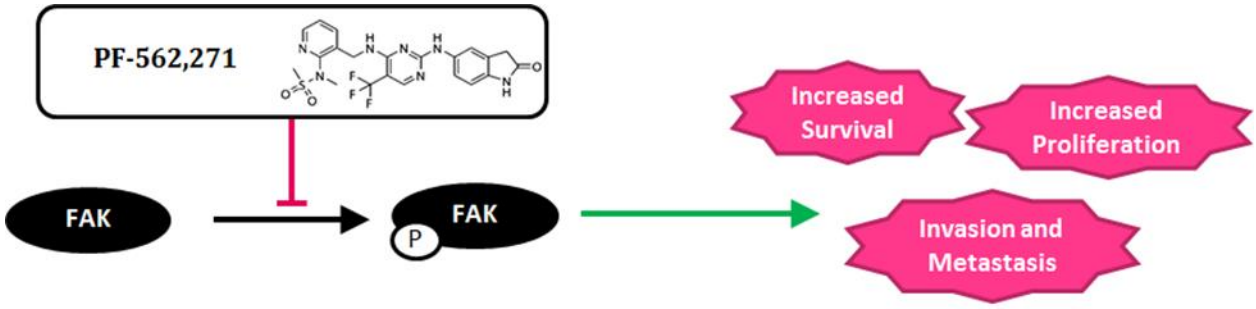

Figure 3: Mechanism of Action for PF-562,271

The commercially available FAK inhibitor PF-562,271 (PF-271) is an ATP mimetic that binds to the ATP binding pocket in the kinase domain of FAK preventing Y397 autophosphorylation and subsequent Src recruitment, thus inhibiting many pathways critical to metastatic behavior and growth.

3.1 PF-271 reduces overall pY397 FAK levels

In order to confirm that the commercial FAK inhibitor PF-271 does in fact decrease pY397 FAK levels, we performed a western blot utilizing various concentrations of PF-271 commonly used when treating breast cancer lines. As shown in **[Figure 4, Panel A]** an overall reduction of pY397 FAK was observed at 48h post-treatment with PF-271, with MDA-MB-231 showing clear dose dependency, in all three cell lines. At the same concentrations of PF-271, a slight reduction in total FAK was also observed in MCF7 and T47D at 5 µM PF-271.However, total FAK levels were not reduced in MDA-MB-231 following drug treatments.

3.2 PF-271 has a similar IC_{50} for all cell lines

Before performing combination treatments with PF-271, it was important to determine what, if any, influence on cell viability PF-271 has as a single agent. Using an MTT assay as a measure of viability, data was collected at 48h post-treatment with varying concentrations of PF-271 for all three cell lines. There is a dose-dependent decrease in viability which plateaus at 5µM at ~23%, as evidenced in **[Figure 4, Panel B]**. All three cell lines produced similar almost overlapping dose dependency curves with comparable IC_{50} concentrations, all of which approximate 3µM PF-271. It is worth noting, as an aside, that a known limitation of MTT, especially at low viabilities that approximate ~20% viability, is that of producing an absorbance which overestimates the percentage of live cells. So while the true IC_{50} may in fact be lower than we have indicated here, what remains unchanged is that PF-271 seems to be affecting their viability equally regardless of the concentration of drug used.

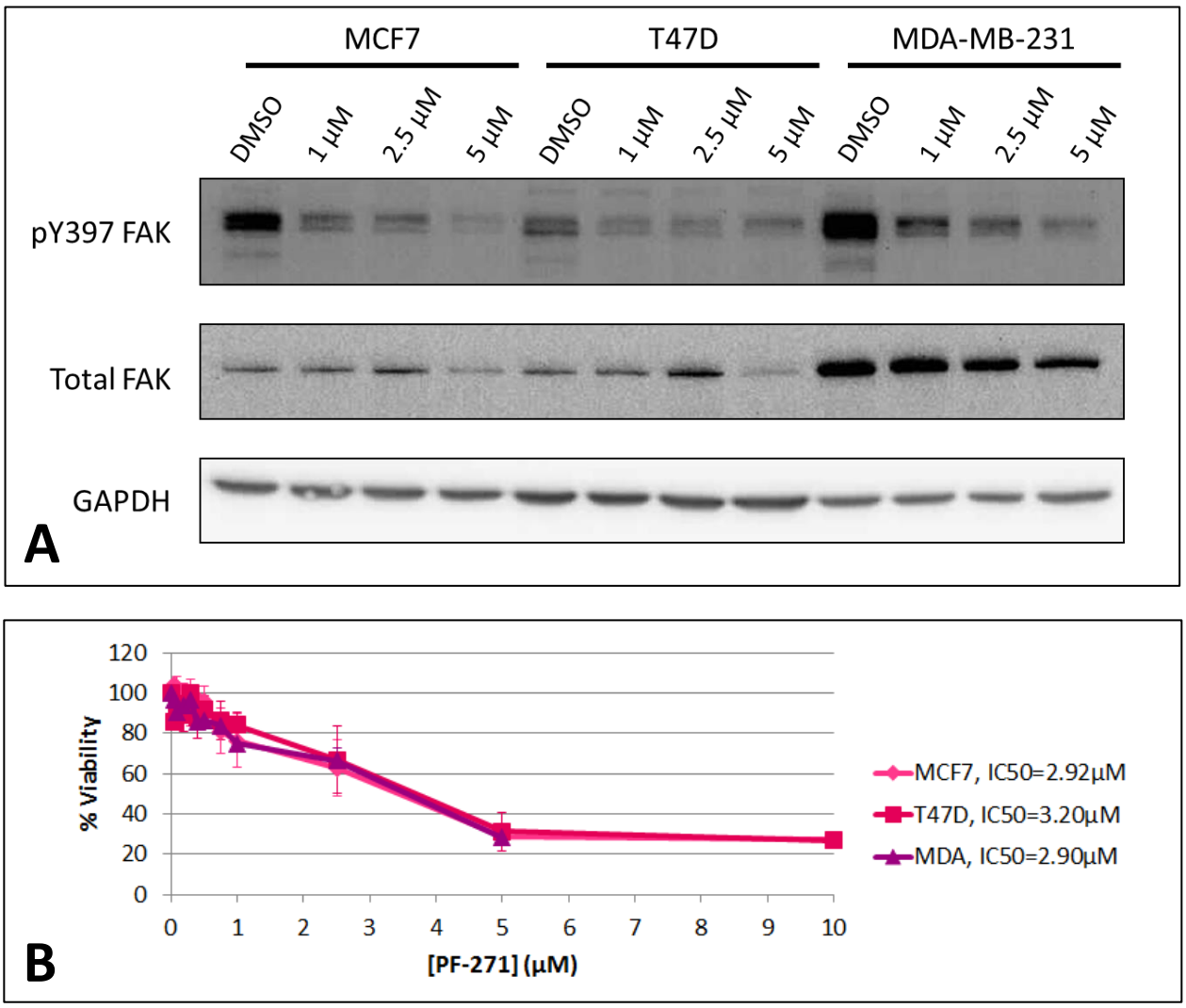

Figure 4: Effects of PF-271 Treatment on Breast Cancer Cells

Panel A, results from a representative western performed at 48h post-treatment showing that PF-271 has ability to specifically reduce pY397 FAK in MDA-MB-231 and seems to degrade total FAK in both MCF7 and T47D. Panel B, results of MTT viability assay performed at 48h post-treatment (n=3, +/- SE) showing little to no difference in IC_{50} concentrations between the three cell lines.

3.3 Preliminary Standard of Care Chemotherapeutic Panel

In order to identify synergistic chemotherapeutic partners for PF-271, cells were treated for 48h with a simultaneous combination of PF-271 and an appropriate experimental chemotherapeutic and viability was assessed using MTT. The chemotherapeutics used in the initial panel are listed in **(Table 3)**. The chemotherapeutic drugs used were selected based on their use as standard-of-care in metastatic breast cancer and also to represent a variety of mechanisms of action. A variety of concentrations of both drugs were used in an attempt to maximize the probability of identifying potential synergistic combinations. The interactions observed for each drug combination can be roughly categorized into three categories: no interaction, antagonistic interaction, additive/synergistic interaction. Further identification of synergy was determined using CompuSyn.

Name	Drug Class	Mechanism of Action
Anastrozole	Aromatase Inhibitor	Inhibits Synthesis of Estrogen (71)
Vinorelbine	Anti-Mitotic	Binds Tubulin and Prevents Microtubule Assembly (72)
Doxorubicin	DNA Damage & DNA Repair Inhibition	Intercalates into DNA and Inhibits Topoisomerase II (73)
Cisplatin	DNA Damage	Forms DNA Crosslinks (74)

Table 3: Compounds used in Preliminary Chemotherapeutics Panel

A list of the compounds used in the preliminary chemotherapeutics drug panel focussing on standard of care, including their drug class and overview of their mechanism of action.

Anastrozole showed no ability to kill cells as a single agent nor enhance or hinder PF-271's ability to inhibit cell viability, even up to 10μM concentrations **(Figure 5, Panel A).** Vinorelbine was shown to have an ability to inhibit cell viability as a single agent, reducing cell viability to ~40% in all cell lines with doses as low as 0.1μM even in the absence of PF-271. However, curiously, when in combination with PF-271, this cytotoxic effect was diminished when the concentration of both drugs

was low. For example, 0.1µM vinorelbine produced ~55% cell viability when combined with 0.5µM PF-271. This antagonistic interaction was reduced at high concentrations of either drug as the cytotoxic effect of either drug appears to becomes too much to be overcome by any antagonistic effect **(Figure 5, Panel B).** Another microtubule inhibitor that was briefly examined, docetaxel, showed similar antagonistic behaviour, but was only tested in MCF7 cells **(See Appendix)**.

Cisplatin showed a modest ability to decrease cell viability as a single agent. However, at certain low concentrations of PF-271, namely 1µM, there appeared to be a potential for modest synergy in MDA-MB-231 **(Figure 6).** When treated with 1µM of both PF-271 and cisplatin, the cell viability achieved was statistically different than using 1µM of PF-271 alone, and approached, but did not quite reach, statistical significance compared to 1µM cisplatin alone in MDA-MB-231 cells. Analysis using CompuSyn, as described in Section 2.4, assigned the relationship a combination index (CI) value of 0.6432; which being <1, indicated moderate synergy. While MCF7 showed no capacity for synergy or additivity whatsoever, there are possibly hints of mild synergy in T47D, with a greater than 10% further decrease in viability when the two drugs are combined. This is in addition to a CI-value of 0.8774, which indicated slight synergy. However, while combination resulted in a statistically significant decrease in cell viability compared to treatment using 1µM of PF-271 alone, the variance in the data resulted in a lack of statistical significance when comparing the combination to 1µM of cisplatin alone. This lack of statistical significance may be partially derived however from the higher statistical power required to discern the less potent synergy exerted in T47D cells (CI=0.8774) as compared to MDA-MB-231 cells (CI=0.6432). Additional replicates may yet produce statistical significance in T47D, but it is inappropriate to provide further speculation without additional investigation.

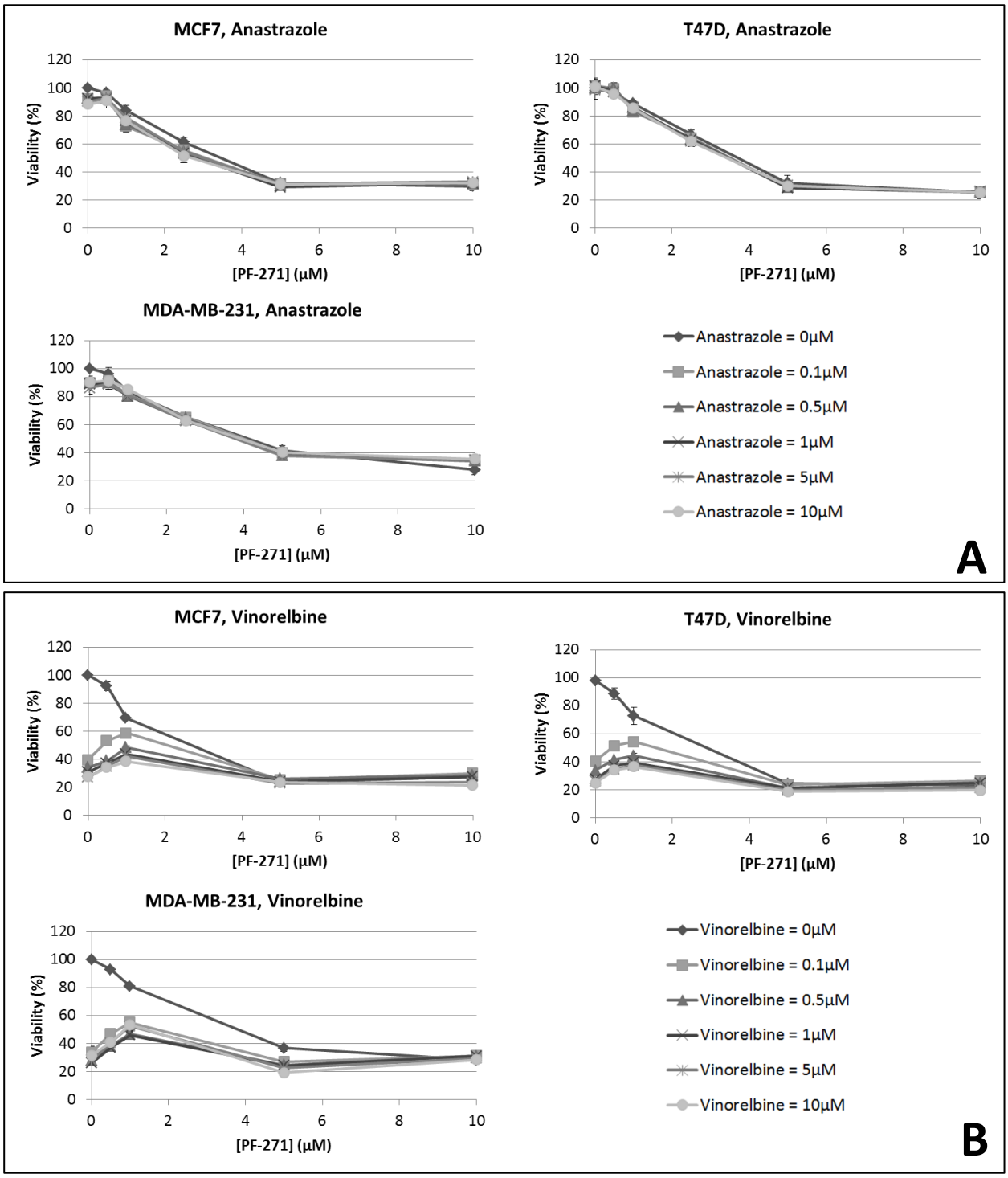

Figure 5: Combinations of PF-271 with Anastrozole and Vinorelbine

Metastatic breast cancer lines treated simultaneously with a gradient of PF-271, and anastrazole (Panel A) or vinorelbine (Panel B) for 48h. Viability was measured using MTT, using DMSO as a vehicle control representing 100% viability. Shown are averages of n=3 biological replicates, +/-SE.

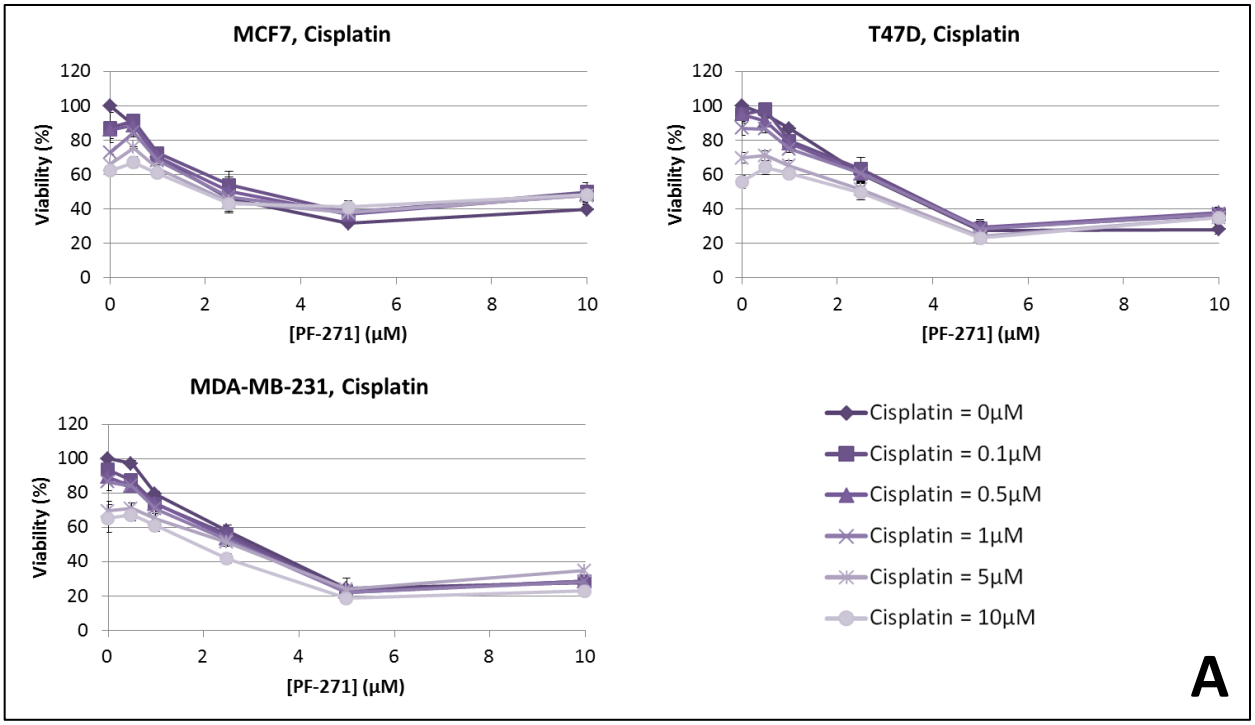

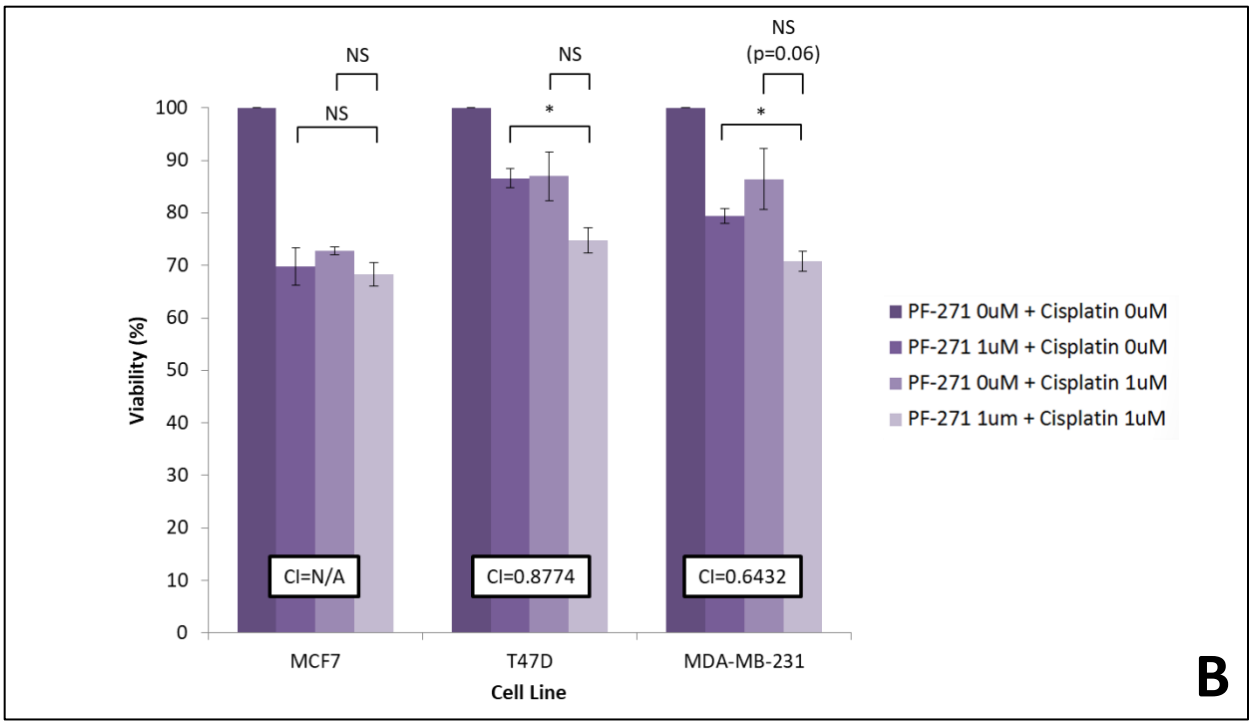

Figure 6: Combinations of PF-271 with Cisplatin

Panel A, metastatic breast cancer lines treated simultaneously with a gradient of PF-271 and cisplatin for 48h. Viability was measured using MTT, using DMSO as a vehicle control representing 100% viability. Panel B, results from a targeted statistical analysis at promising concentrations. Combination index values are listed above each cell line. Analysis was not performed for MCF7 due to insufficient statistical significance. Shown are averages of n=3 biological replicates, +/-SE.

The other DNA damaging agent examined in our preliminary assessment, doxorubicin, shows a more potent ability to reduce cell viability as a single agent. It also shows an increased potential for additivity or synergy when combined with PF-271 **(Figure 7)**. Incidentally, the doses showing the largest combinatorial decrease in cell viability, and therefore those doses most likely to produce a CI-value of equal to or less than 1 upon further analysis, were detected using 2.5µM PF-271 and 0.1µM of doxorubicin in all three cell lines. Upon further analysis, potential for moderate synergy was detected, with a CI-Value of 0.839, along with statistically significant and nearly statistically significant differences compared to treatment with PF-271 and doxorubicin alone respectively for MCF7. In T47D, classical additivity was observed with a CI-value of 1.000, in addition to a statistically significant decrease in cell viability in combination when compared to either drug in isolation. Upon ANOVA analysis, the data for MDA-MB-231 revealed no statistical difference between the viability of cells treated with both compounds in combination compared to or either drug in isolation, so CompuSyn analysis was not performed.

.

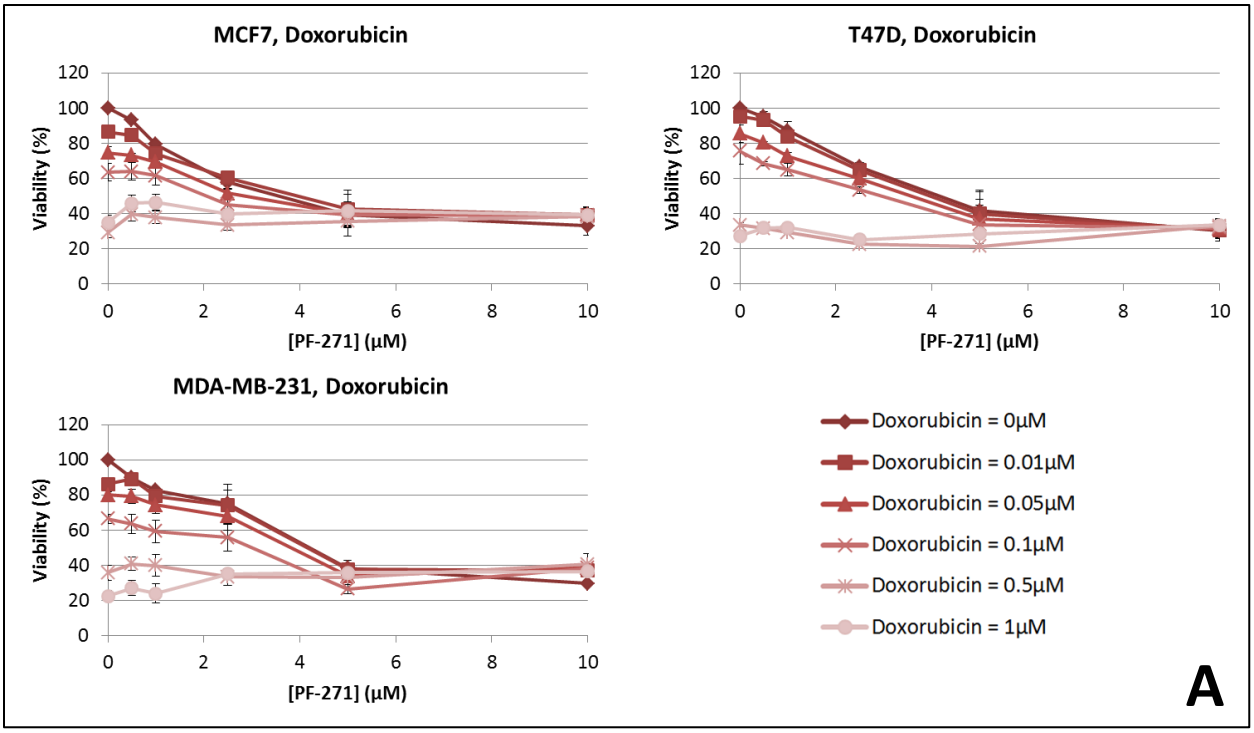

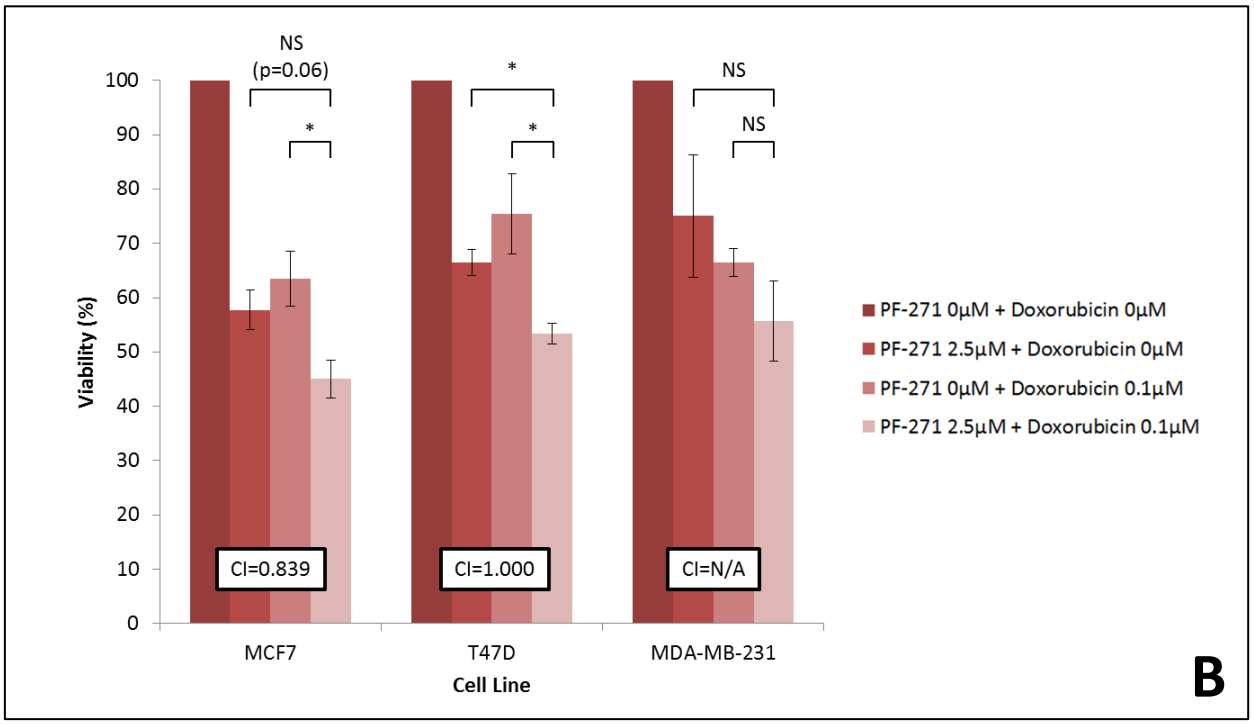

Figure 7: Combinations of PF-271 with Doxorubicin

Panel A, metastatic breast cancer lines treated simultaneously with a gradient of PF-271 and doxorubicin for 48h. Viability was measured using MTT, using DMSO as a vehicle control representing 100% viability. Panel B, results from a targeted statistical analysis at promising concentrations. Combination index values are listed above each cell line. Analysis was not performed for MDA-MB-231 due to insufficient statistical significance. Shown are averages of n=3 biological replicates, +/-SE.

3.4 Secondary DNA-Damaging Agent Only Panel Reveals Topoisomerase Inhibitor-Specific Synergy with PF-271

With the results of the preliminary panel suggesting that the inhibition of FAK activity may promote synergy when used with DNA damaging agents, additional DNA damaging agents were acquired and subjected to similar combination assays to probe for a more efficacious synergistic partner for PF-271. Again, focus was placed on standard-of-care drugs as well as those representing a variety of mechanisms of action **(Table 4)**.

Name	Drug Class	Mechanism of Action
Etoposide	DNA Repair Inhibition	Topoisomerase II Inhibitor (75)
Topotecan	DNA Repair Inhibition	Topoisomerase I Inhibitor (76)
5-Fluorouracil	Antimetabolite	Inhibition of Thymidylate Synthase (15)
Cyclophosphamide	DNA Damage	Forms DNA Crosslinks (77)

Table 4: Compounds used in Secondary Chemotherapeutics Panel

A list of compounds used in secondary DNA damage-specific chemotherapeutics drug panel. Includes drug class and overview of their mechanism of action.

5-Fluorouracil showed modest cytotoxic effects when used as a single agent; however there was no significant potential for synergy or additivity detected in any cell line upon further review via CompuSyn when used in combination with PF-271 **(Figure 8, Panel A)**. Cyclophosphamide showed similar behavior to anastrazole, where it showed no capacity to inhibit growth as a single agent, nor did it result in decreased cell viability when combined with PF-271 **(Figure 8, Panel B)**.

However, both etoposide and topotecan showed a similar potential for synergy in combination with PF-271 as was previously seen with doxorubicin. This is of particular interest as doxorubicin, etoposide and topotecan are all topoisomerase inhibiting agents, with doxorubicin and etoposide

inhibiting topoisomerase-II and topotecan inhibiting topoisomerase-I. Closer statistical examination of etoposide revealed that 2.5μM PF-271 combined with 1μM etoposide likely promoted synergy in all cell lines. The combination in T47D cells showed significance when compared to either drug in isolation, and both MCF7 and MDA-MB-231 showed similar effects that trended toward significance **(Figure 9)**. Using 2.5μM PF-271 and 0.5μM topotecan in combination produced an even more pronounced effect and all cell lines exhibited moderate synergy (CI<0.7) showing significantly more potent inhibition with both drugs in combination as compared to either drug alone. Only the MCF7 cell line falls just short of statistical significance, with every other cell line showing strong statistically significant decreases in cell viability **(Figure 10)**.

Topotecan was, therefore, selected for further investigation as a model topoisomerase inhibitor due to its consistent and comparatively potent synergistic effect across the all three cell lines as compared to the other chemotherapeutics examined thus far.

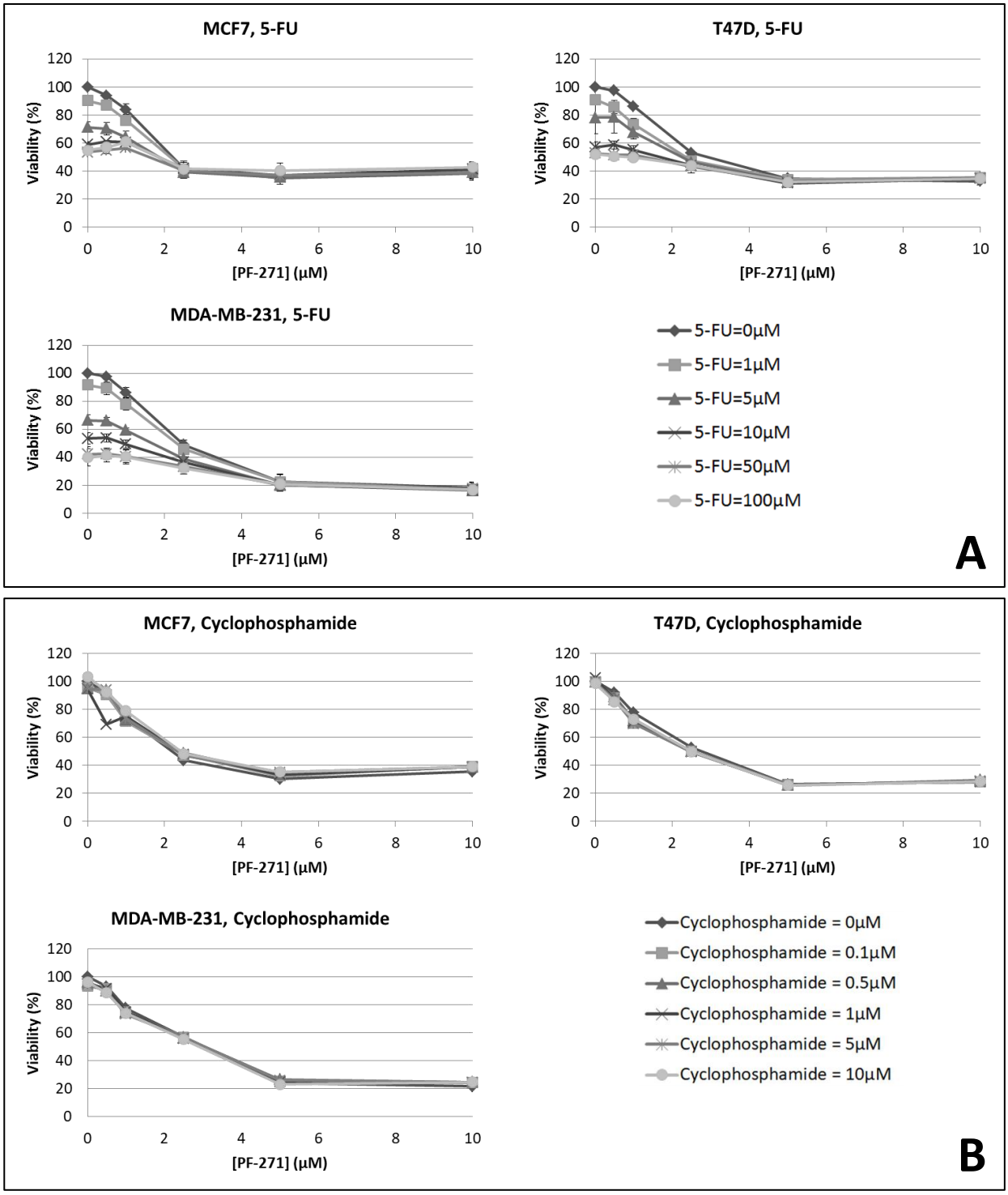

Figure 8: Combinations of PF-271 with 5-Fluorouracil and Cyclophosphamide

Metastatic breast cancer lines treated simultaneously with a gradient of PF-271, and 5-fluorouracil (5-FU) (Panel A) or cyclophosphamide (Panel B) for 48h. Viability was measured using MTT, using DMSO as a vehicle control representing 100% viability. Shown are averages of n=3 biological replicates, +/-SE.

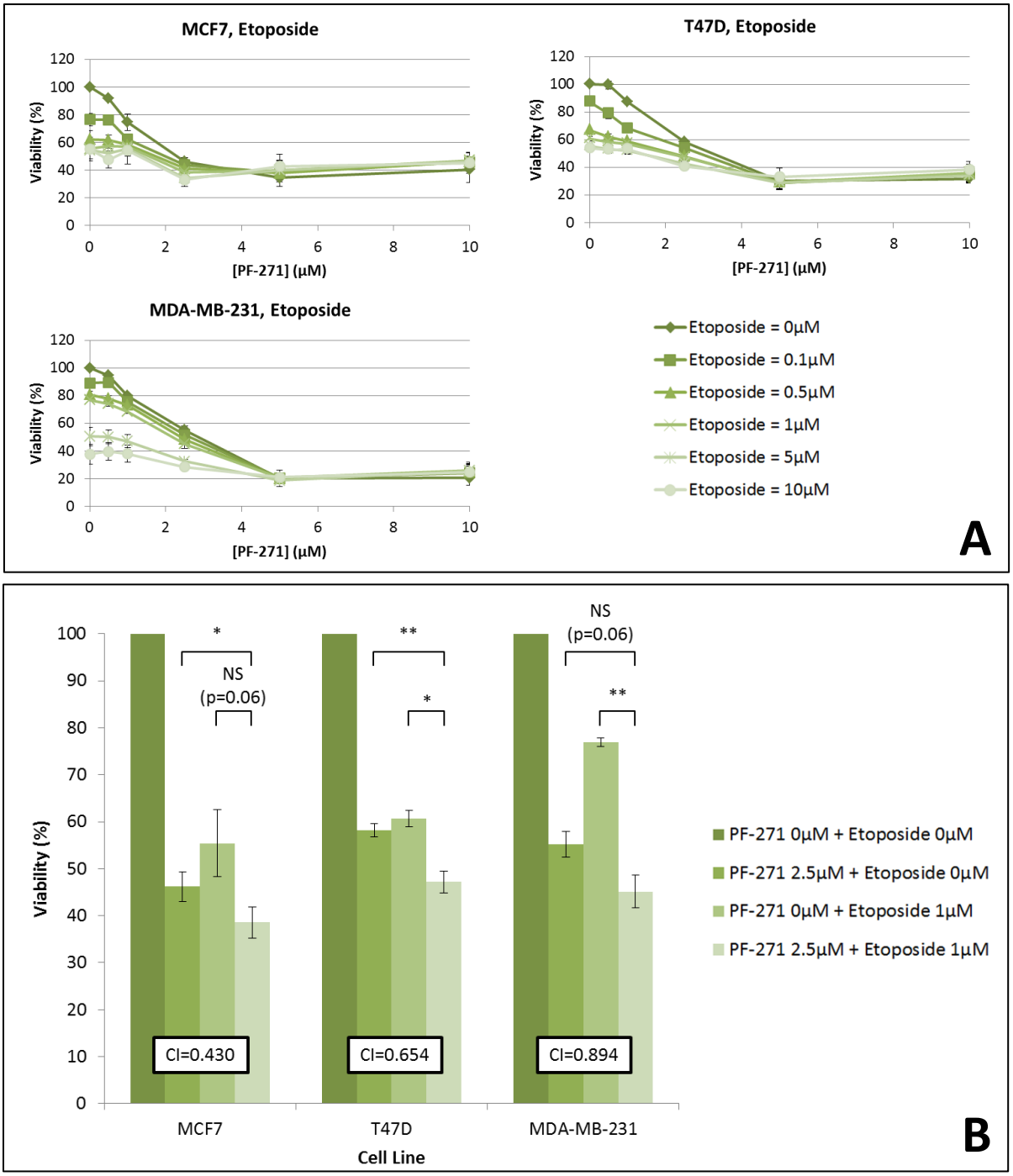

Figure 9: Combinations of PF-271 with Etoposide

Panel A, metastatic breast cancer lines treated simultaneously with a gradient of PF-271 and etoposide for 48h. Viability was measured using MTT, using DMSO as a vehicle control representing 100% viability. Panel B, results from a targeted statistical analysis at promising concentrations. Combination index values are listed above each cell line. Shown are averages of n=3 biological replicates, +/-SE.

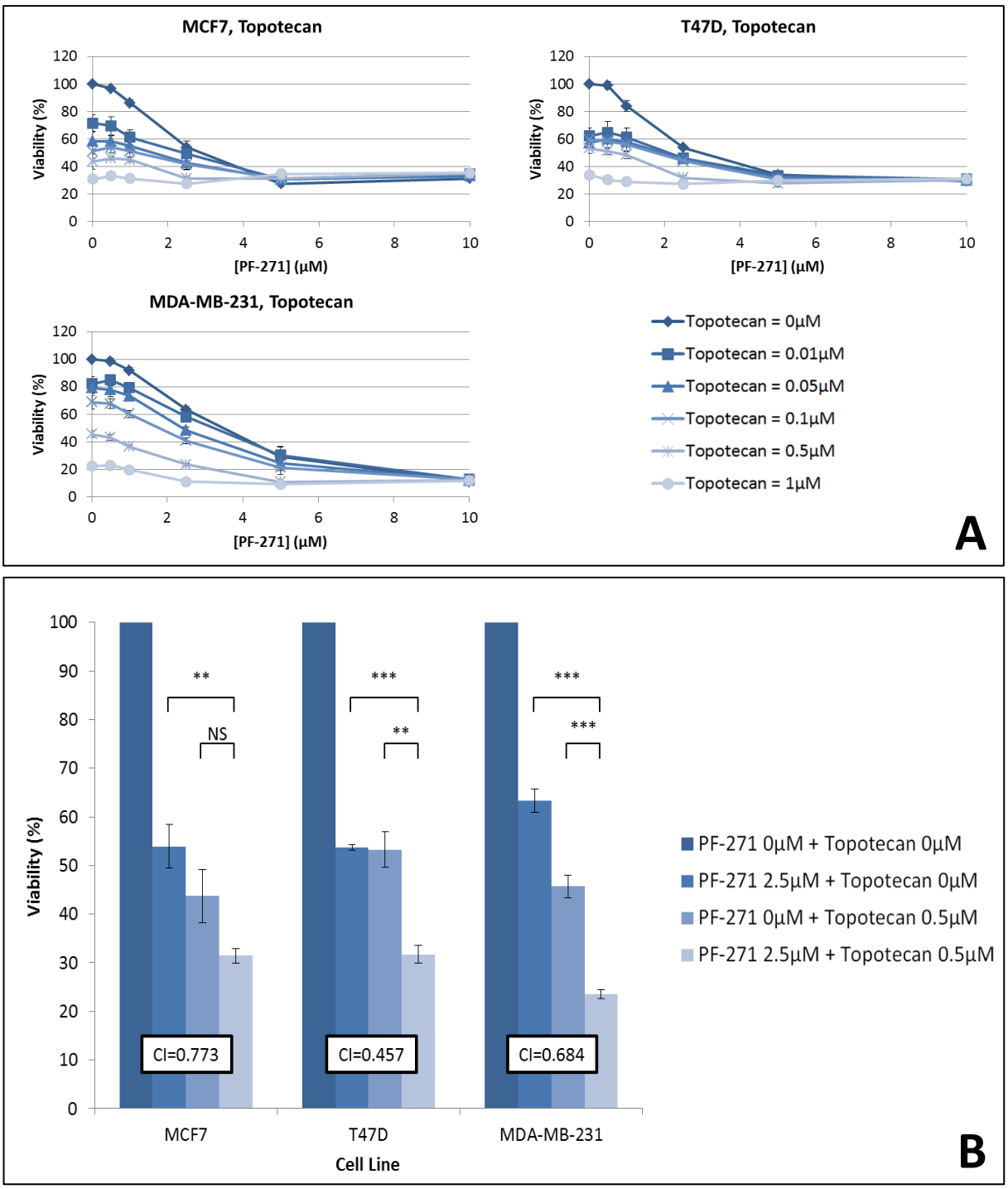

Figure 10: Combinations of PF-271 with Topotecan

Panel A, metastatic breast cancer lines treated simultaneously with a gradient of PF-271 and topotecan for 48h. Viability was measured using MTT, using DMSO as a vehicle control representing 100% viability. Panel B, results from a targeted statistical analysis at promising concentrations. Combination index values are listed above each cell line. Shown are averages of n=3 biological replicates, +/-SE.

3.5 Flow Cytometry Reveals Differing Mechanisms of Action for Topoisomerase Inhibitors vs. PF-271

In an attempt to confirm the potential synergistic inhibition of cell viability implied by the MTT assay results, we initiated studies to determine if increased rates of apoptosis were observed in cells treated with both PF-271 and topotecan in isolation and in combination. Relative DNA content was assessed using PI staining and flow cytometry analysis on all cell lines after treatment with each drug in isolation and in combination in order to determine the proportion of cells undergoing apoptosis using SubG1 measurement. Control cells treated with DMSO showed a typical high 2n peak followed by a 4n peak of smaller magnitude, indicating typically cycling cells **(Figure 11).** Treatment with PF-271 produced a increase in the percentage of SubG1 cells in all cell lines, with the increase being dose-dependent in T47D and MDA-MB-231 cells, and plateauing at around three-fold increase in MCF7 **(Figure 12)**. This increase in SubG1 was also accompanied by a shift in the histogram profile, which seemed to favour a higher magnitude 4n peak, implying a G2/M cell cycle arrest. Treatment with topotecan produced a similar, but more potent, increase in SubG1 cells in all three cell lines, with the same dose dependency pattern as before for the three cell lines. However, topotecan was far more effective at inducing this response in T47D and MDA-MB-231 cells, producing upwards of 36% and 49% SubG1 cells with 1µM, respectively. The increase in SubG1 cells relative to baseline for MCF7 was more modest at approximately 10%, twice as high as the baseline 4%. This increase in SubG1 was accompanied by a distinct spike in 2n cell population, implying an arrest at G1/S. The combination doses of 2.5µM PF-271 and 0.5µM topotecan respectively produced no additive or synergistic increase in the SubG1 cell population, and appear to show a hybrid histogram indicating both G1/S arrest and increased G2/M arrest.

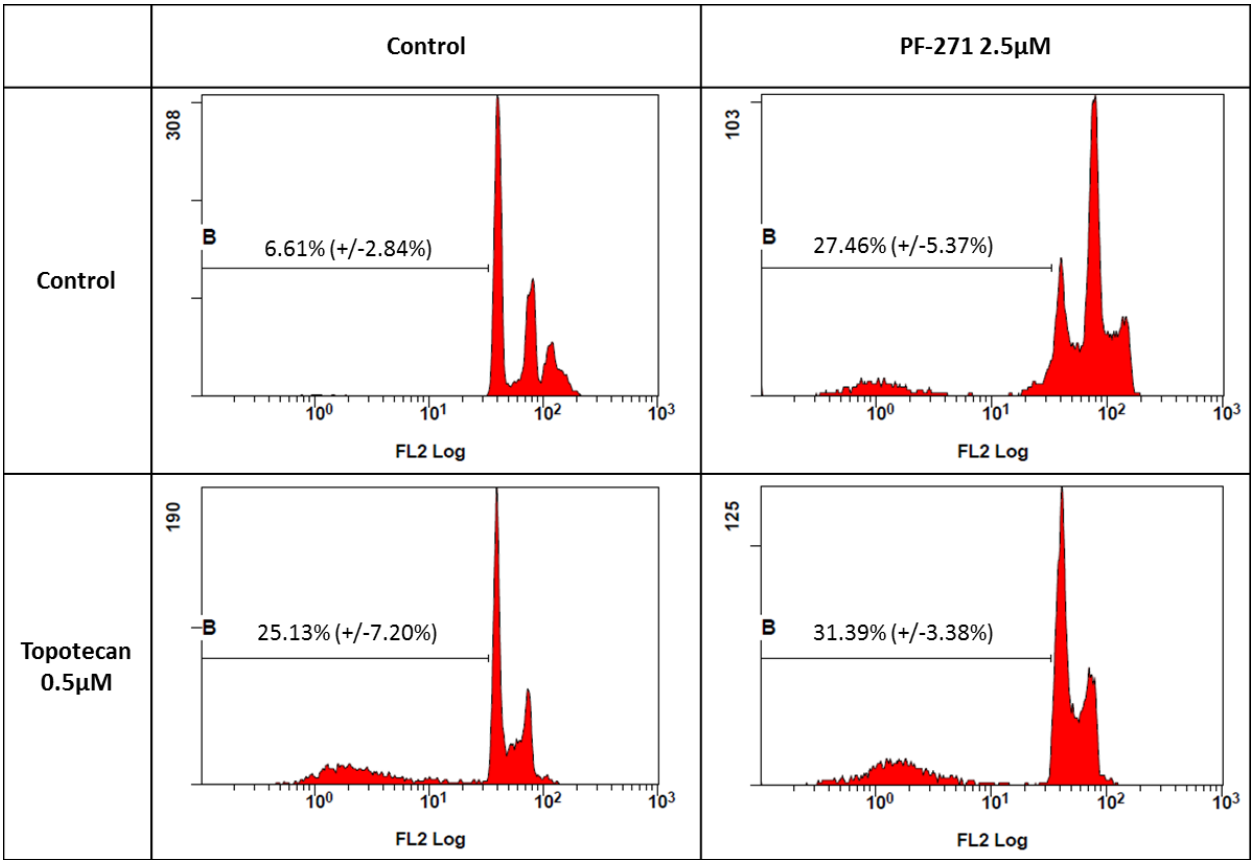

Figure 11: Flow Cytometry Histograms of PF-271 and Topotecan Treated Cells

Example of gated flow cytometry analysis of PI stained T47D following 48h treatment with PF-271 and topotecan. Numbers listed indicate the percentage of SubG1 cells (+/- SE) Note the distinct 4n peak following PF-271 treatment, 2n peak following topotecan treatment and intermediate response during combination treatment. Similar data was derived from MCF7 and MDA-MB-231 cells. Figures shown are representative, but %SubG1 values derived from n=2, with two technical replicates per biological replicate.

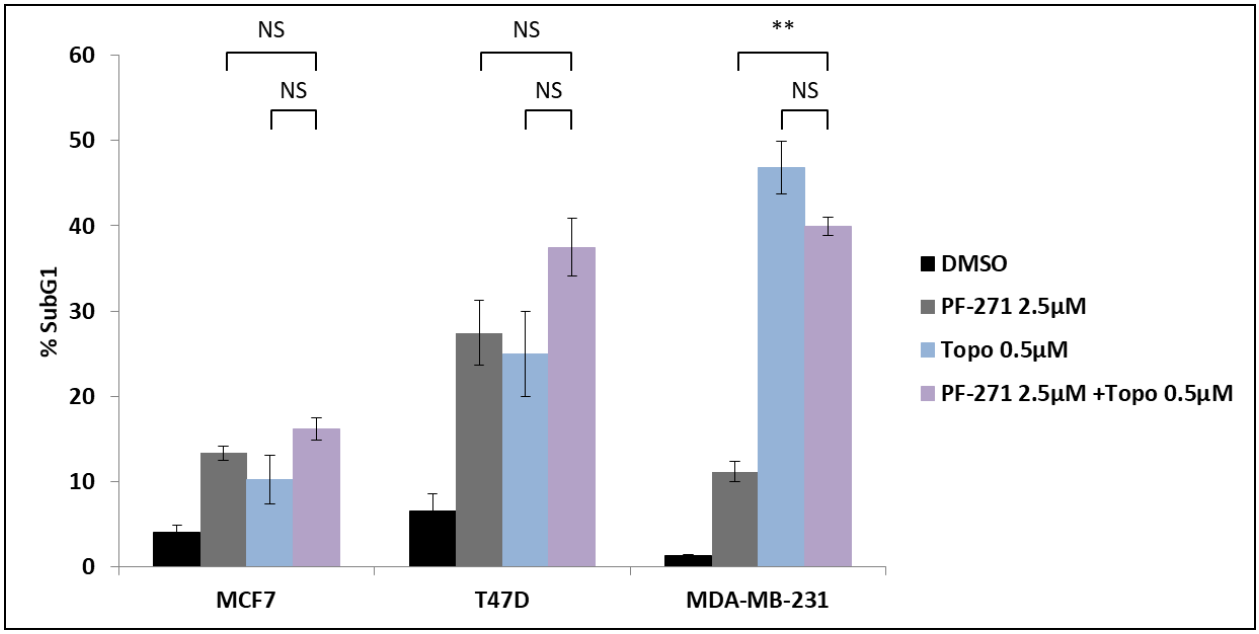

Figure 12: Quantification of SubG1 Cells in PF-271 and Topotecan Treated Cells

Results showing average percentage of cells showing SubG1 DNA content following 48h treatment with varying concentrations of PF-271, topotecan, or a combination of both drugs. Combination concentrations used reflect those which showed synergistic decrease in cell viability via MTT. Averages of n=2, +/- SE shown.

This pattern also exists in preliminary flow cytometry analysis at varying concentrations of both drugs in combination **(Figure 13)**. While there is potential for increased SubG1 levels at select concentrations of PF-271 and topotecan for T47D (PF-271 1µM & 1µM topotecan), as well as in MDA-MB-231 (1µM & 0.1µM, 2.5µM & 0.1µM, 5µM & 0.1µM, and 5µM & 0.5µM of PF-271 and topotecan respectively) relative to either drug alone, the increase is slight (<5% change in most cases) and may simply be due to variability in the sample. The majority of the combinations analysed showed no relative increase in SubG1 when compared to treatment with similar concentrations of either drug alone. However it is worth noting that the results shown are for an n=1, and may yet show a statistically significant difference upon further analysis. However, at this stage, the preliminary results corroborate that of the other flow cytometry data.

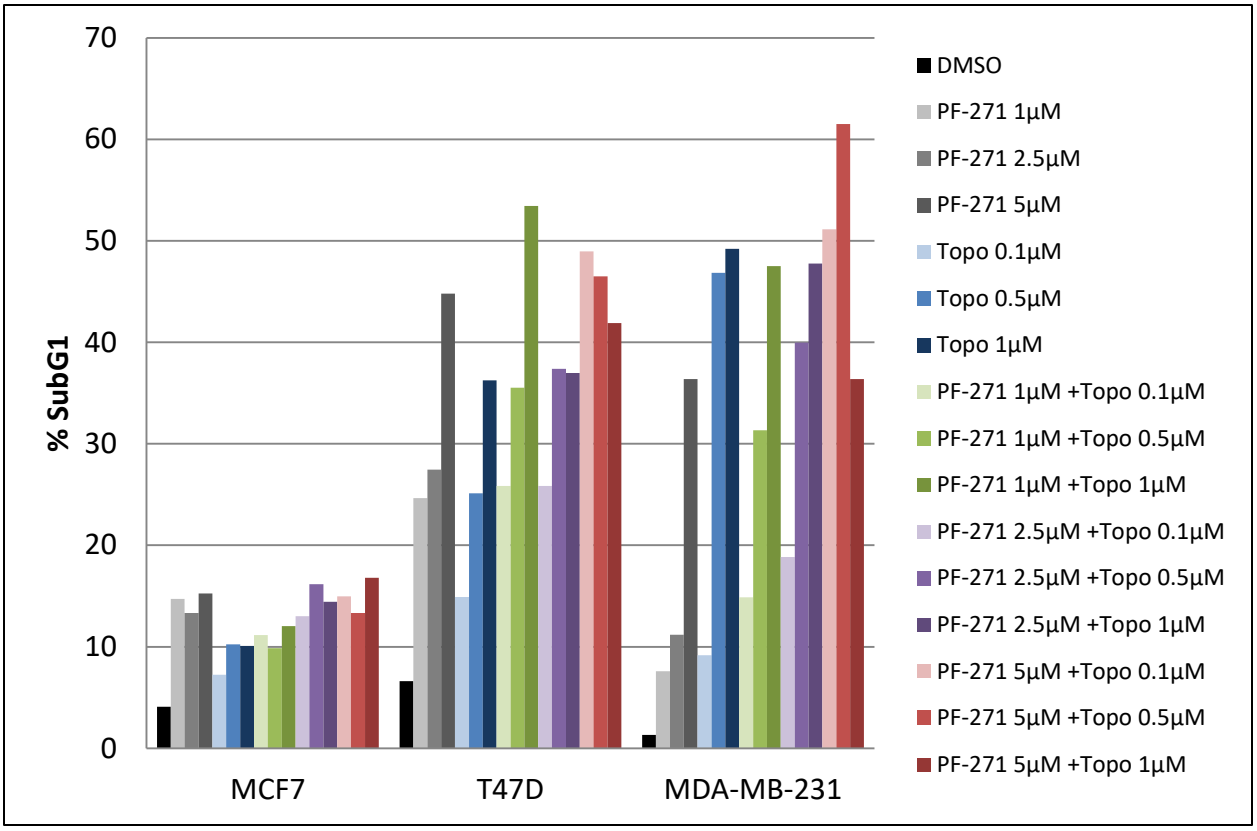

Figure 13: Further Quantification of SubG1 Cells in PF-271 and Topotecan Treated Cells

Preliminary results showing average percentage of cells showing SubG1 DNA content following 48h treatment with varying concentrations of PF-271, topotecan, or a combination of both drugs. Results shown are of an n=1 performed in duplicate.

3.6 No Significant Decrease in Cell Number

Due to the discrepancy between the cell viability data derived from the MTT assay and the apoptosis data derived from flow cytometry analysis, another measure of cell viability, a trypan blue exclusion assay, was performed. Cells treated with combinations of topoisomerase inhibitor and PF-271 that were shown to produce synergistic decreases in cell viability via MTT were subsequently re-examined using the trypan blue assay **(Figure 14)**. The three topoisomerase inhibitors were examined in this context, and treatment with each drug in isolation showed a decrease in cell number relative to baseline DMSO vehicle control treated cells for each cell line. This decrease in cell number was also observed following single agent PF-271 treatment as well, which corroborates earlier observations via MTT. When combined however, none of the combinations produced a statistically significant knockdown in cell number relative to either drug in isolation. To confirm however, further trypan blue assays were performed using higher concentrations of topotecan, and no such synergistic decrease in cell number was observed **(Figure 15)**.

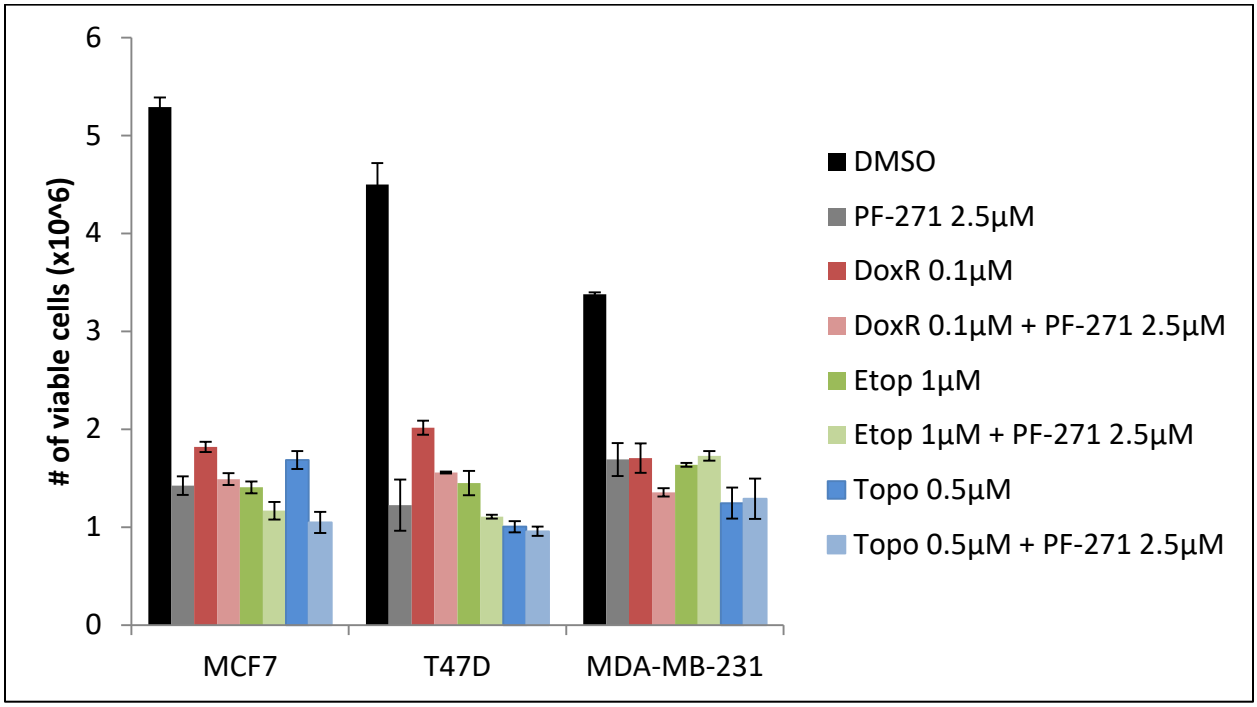

Figure 14: Proliferation Assay Following Treatment with PF-271 and Topoisomerase Inhibitors

Proliferation assessed via trypan blue exclusion assay to count the number of viable cells 48h post-drug treatment. DoxR=doxorubicin, Etop= Etoposide, Topo=Topotecan. Averages of n=3, +/-SE are shown.

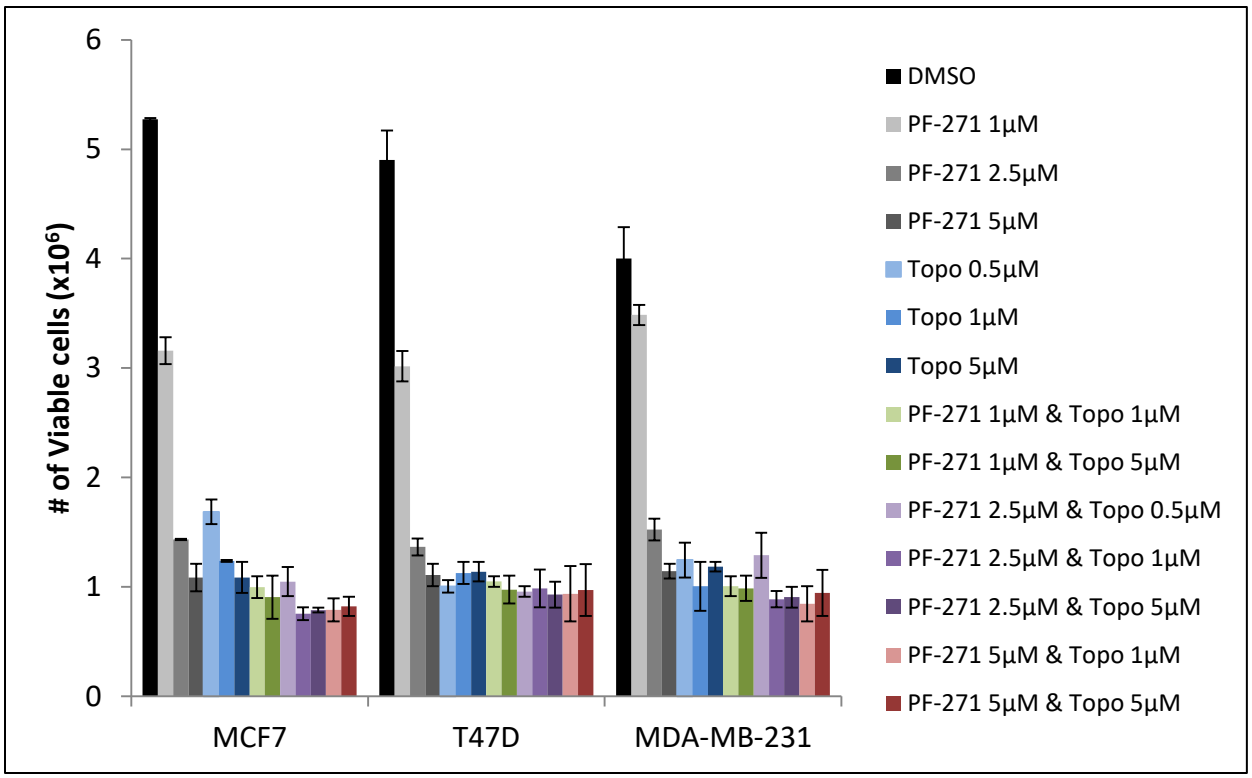

Figure 15: Proliferation Assay of PF-271 and Various Concentrations of Topotecan

Proliferation assessed via trypan blue exclusion assay to count the number of viable cells 48h post-drug treatment. Topo=Topotecan. Averages of n=2, +/-SE are shown.

3.7 Preliminary Results Indicate Topotecan Induces pFAK Expression

Given the conflicting data regarding the MTT and trypan blue assay data, we endeavoured to determine if the conflicting data is derived from an unexpected side effect of the topoisomerase inhibitors. An unanticipated change in protein levels or cellular metabolism could affect MTT readout (78). With this in mind, we focused on what impact, if any, topotecan has on FAK activity and levels.

Western analysis of cells, treated for 48h with PF-271 showed the expected decrease in pY397 FAK levels relative to total FAK which remained consistent **(Figure 16)**. However, treatment with topotecan in isolation produced an increase in pY397 FAK levels in a dose-dependent manner. Any increase appears to be negated when PF-271 and topotecan are used in combination though **(Figure 17)**. However, at 6h, **(Figure 17)** does not replicate the dose dependant increase in pY397 FAK observed in **(Figure 16)**. It should therefore be noted that these results are products of a single replicate, and are therefore extremely preliminary, so any conclusions drawn should be regarded with caution. Further analysis will be performed at a later date.

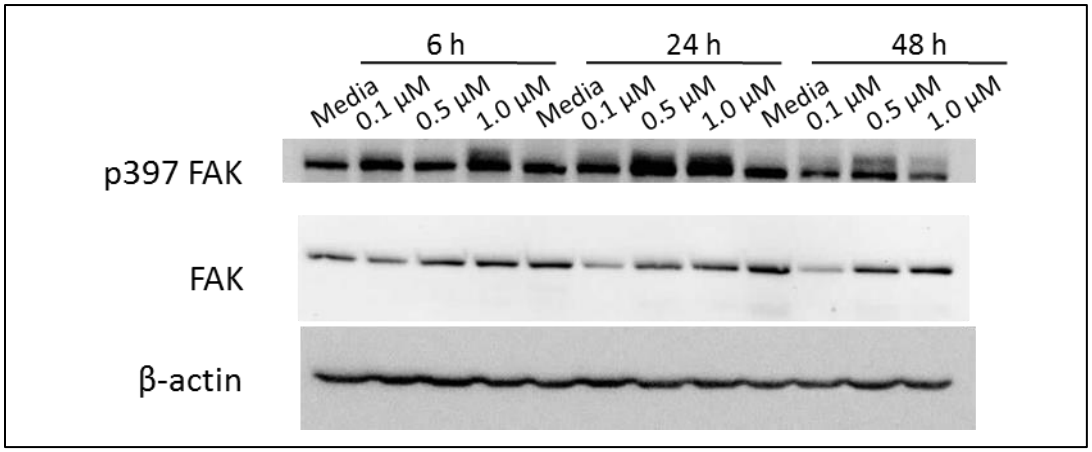

Figure 16: Western Analysis of Topotecan Treated T47D

Western analysis of T47D cells with increasing concentrations of topotecan at varying time points. Performed by Viya Vijithakumar. Preliminary n=1 shown.

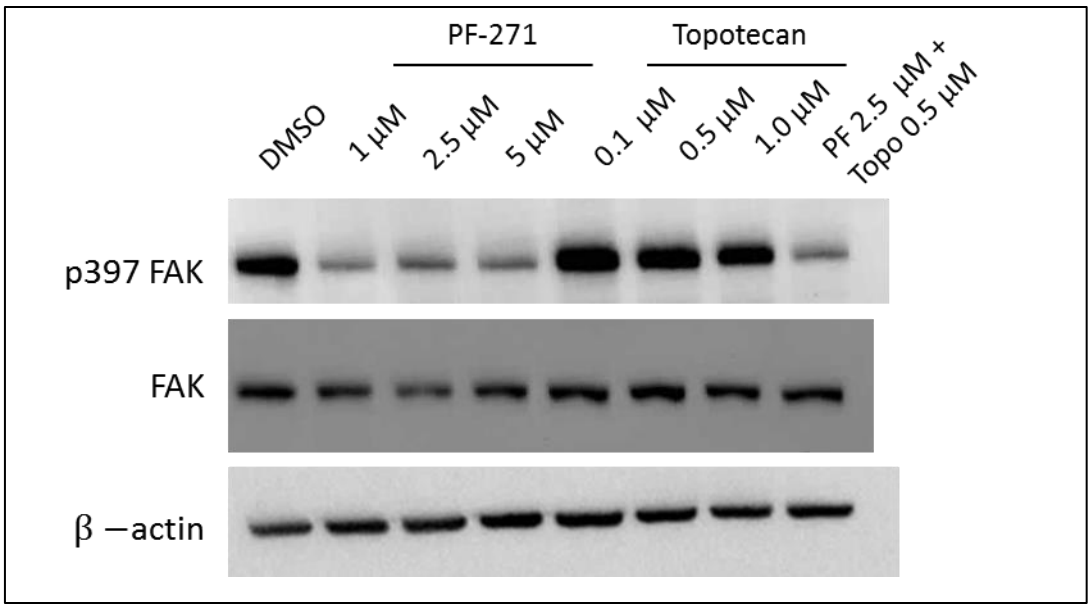

Figure 17: Western Analysis of PF-271 and Topotecan Treated Cells

Western analysis of T47D cells at 6h treated with increasing concentrations of PF-271 and topotecan as well as a combination of both drugs (right-most lane).Performed by Viya Vijithakumar. Preliminary n=1 shown.

3.8 No Significant Decrease in Survival Signal Expression

In order to determine if the combination of topotecan with a FAK inhibitor was inducing a compensatory survival response, we examined the expression of survival signals Bcl2 and Bcl-L1 in response to treatment as both are known to be affected by FAK expression **(Figure 18)** (79) (80). At the relatively early time point of 6h post-treatment with PF-271, Bcl2 appears to show a modest dose dependent decrease in mRNA expression of 20-40% relative to baseline following treatment with doses greater than 2.5 µM in all three cell lines. In response to topotecan, MCF7 and T47D also showed a consistent dose dependent decrease in Bcl2 expression, whereas MDA-MB-231 showed an increase at low PF-271 followed by a sharp decrease which plateaus at ~25% baseline expression at 0.5µM topotecan.

Bcl2-L1 levels follow a similar pattern with typically dose-dependent decreases in expression levels as the concentrations of both drugs increase. Bcl2-L1 shows a dose dependant decrease in expression following increasing levels of PF-271 in all cell lines. There is a potential increase in Bcl2-L1 at low levels of topotecan (0.1µM) in MCF7 and T47D. However, this increase is modest (approximately 40% increase in for both cell lines), and is not replicated in MDA-MB-231 cells. Regardless, as the concentration of topotecan increases, expression of Bcl2-L1 decreases, similar to what was observed with Bcl2.

No combination effect was detected for either Bcl2 or Bcl2-L1 when both compounds were used at concentrations that produced the earlier synergistic decrease in cell viability.

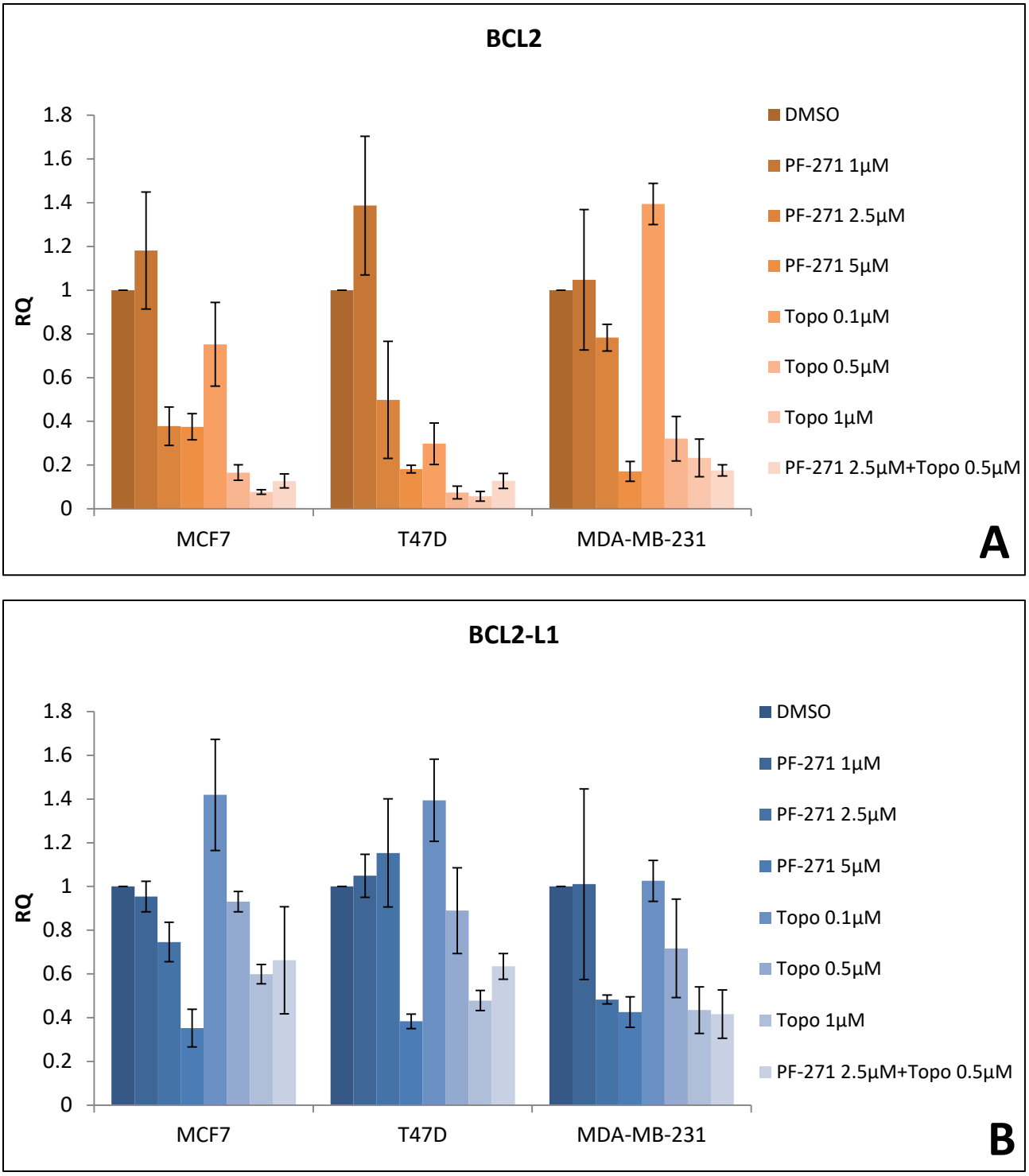

Figure 18: Survival Signal Expression Following PF-271 and Topotecan Treatment

qPCR analysis of Bcl2 (Panel A) and Bcl2-L1 (Panel B) mRNA expression levels following 6h treatment with PF-271 and topotecan. Results from n=3 shown, +/- SE.

3.9 Topotecan and PF-271 Induce Reactive Oxygen Species Production

While an MTT assay is often used as a proxy for measuring the number of viable cells, in truth it is more accurately described as a measure of cellular metabolism. The method relies on the conversion of MTT to formazan via NADPH-dependant enzymes (78) Therefore, in order to investigate possible mechanisms of action for the synergistic decrease in metabolism observed via MTT, we decided to delve into a known metabolic by-product of topoisomerase inhibitors, reactive oxygen species (ROS) (81). ROS levels were measured using high performance liquid chromatography (HPLC) which measures the production of both superoxide and other non-specific ROS via the degradation of the dye dihydroethidium (DHE) into 2-hydroethidium (2OHEth) or into ethidium (Eth) via superoxide or non-specific ROS (such as H_2O_2) respectively. A shorter time point, 6h in this case, was chosen due to the fact that extended exposure to the drugs induces cell death, which would adversely affect HPLC analysis, and 6h would provide ample time for any metabolic impacts of the drugs to be observed with relative ease.

Due to the variability and the sensitivity required for HPLC analysis, in combination with the statistical power required for multiple comparisons testing, we were unable to statistically prove the increase in ROS commonly associated with topotecan treatment, nor that there was any increase in ROS associated with treatment with PF-271 **(Figure 19).**

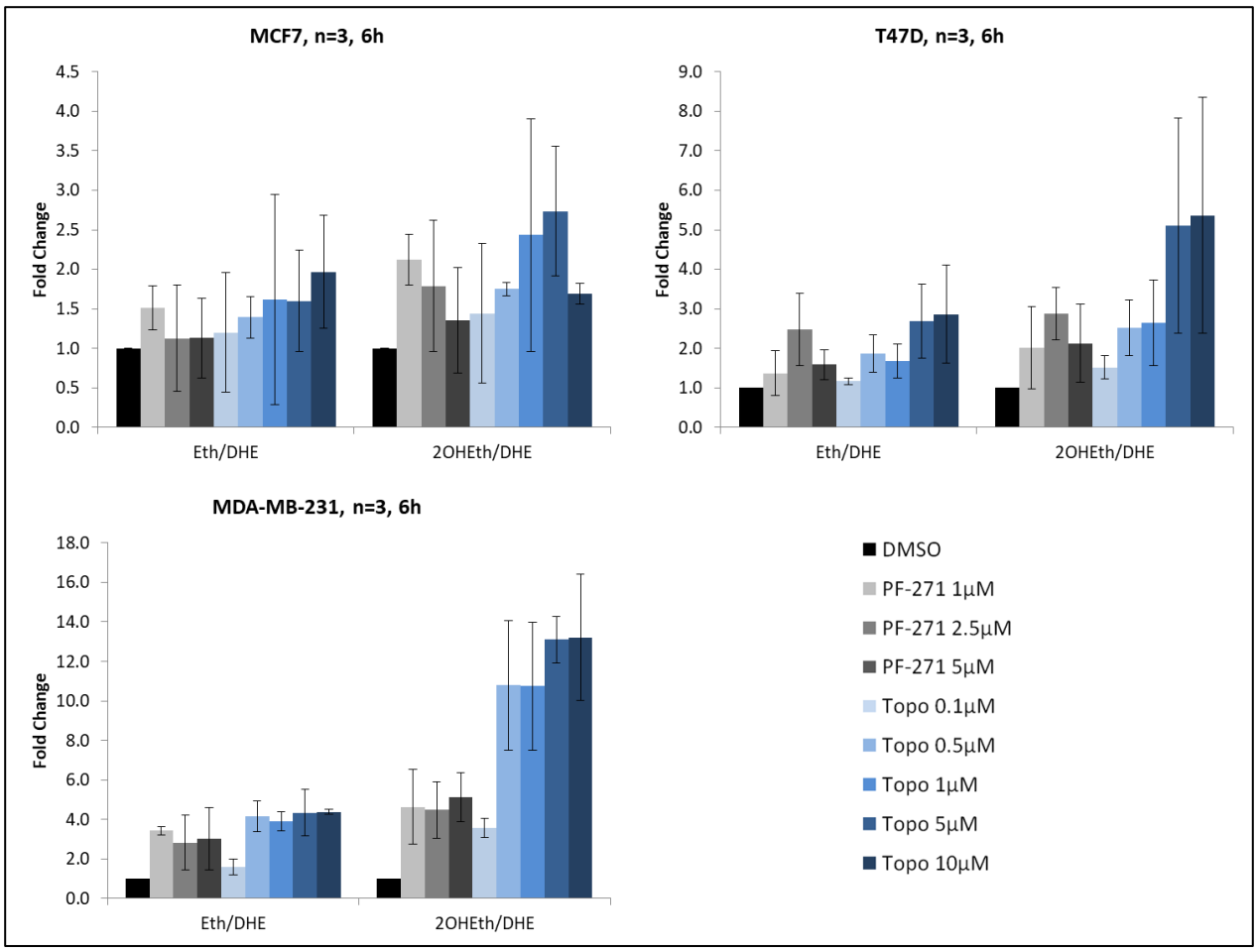

Figure 19: ROS Accumulation Following Individual PF-271 and Topotecan Treatment

HPLC analysis of MCF7, T47D and MDA-MB-231 cells following 6h treatment with PF-271 and topotecan. Ratios of ethidium : dihydroethidium (Eth/DHE) and 2-hydroxyethidium : dihydroethidium (2OHEth/DHE) are listed. Results shown are derived from an average of n=3, +/- SE.

However, treatment with various combinations of both PF-271 and topotecan resulted in a marked increase in ROS relative to DMSO control in all cell lines, albeit at different concentrations of each drug in each cell line. In MCF7 cells, a concentration of 2.5µM PF-271 and 10µM of topotecan produced an approximately 3.5-fold increase in non-specific ROS (as evidenced by the increase in Eth/DHE) and a 6-fold increase in superoxide relative to DMSO **(Figure 20).** This increase was also markedly higher than the levels of ROS observed with treatment of either PF-271 or topotecan alone, with all relevant comparisons producing p-values of a maximum of 0.06 to <0.001. There were similar results for MDA-MB-231 cells treated with 2.5µM PF-271 and 0.5µM topotecan, whose relevant comparative p-values ranged from a maximum of 0.08 to >0.0001 **(Figure 21)**. The increases in ROS observed in the combination treatments were far higher, with an approximately 15-fold and 24-fold increase in non-specific ROS and superoxide respectively compared to baseline. Due to the highly sensitive nature of HPLC, large variability was observed in T47D cells treated with 5µM PF-271 and 5µM topotecan **(Figure 22)**. However, we can state that there is a high probability that there is an approximately 7-fold increase in non-specific ROS as compared to DMSO-treated or PF-271 alone-treated cells as the statistical probabilities trend towards significance (relevant p-values range from a maximum of 0.08 to 0.007). While we cannot conclusively identify the 17-fold increases in superoxide as being statistically distinct from treatment with topotecan alone, it does produce an increase in superoxide relative to DMSO or PF-271 treated cells, in keeping with the pattern observed in other cell lines.

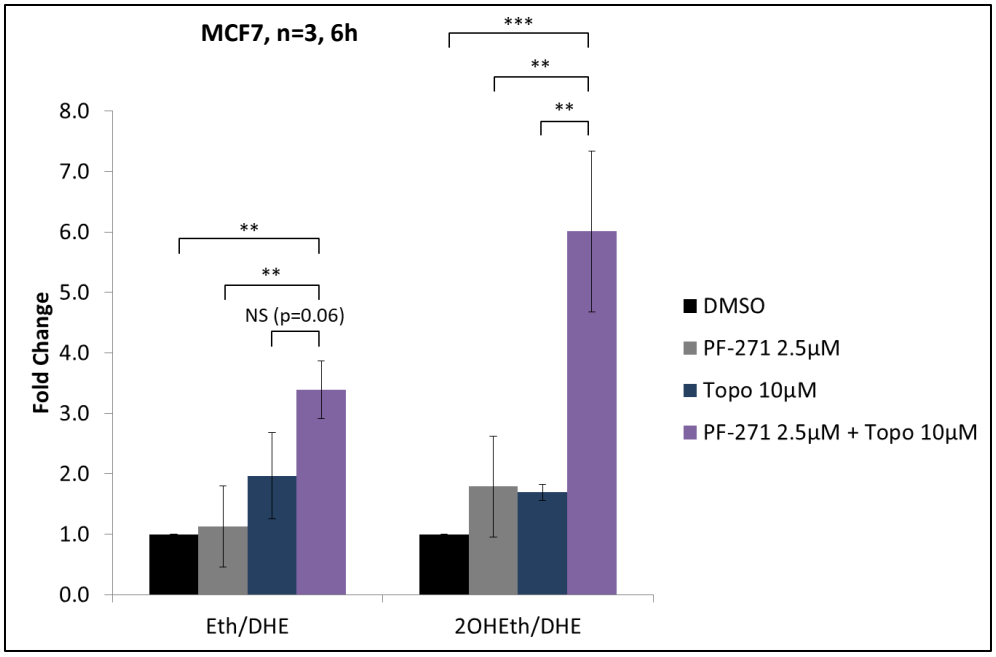

Figure 20: ROS accumulation in MCF7 following Combination PF-271/Topotecan Treatment

HPLC analysis of MCF7 cells following 6h treatment with PF-271 and topotecan. Ratios of ethidium : dihydroethidium (Eth/DHE) and 2-hydroxyethidium : dihydroethidium (2OHEth/DHE) are listed. Results shown are derived from an average of n=3, +/- SE.

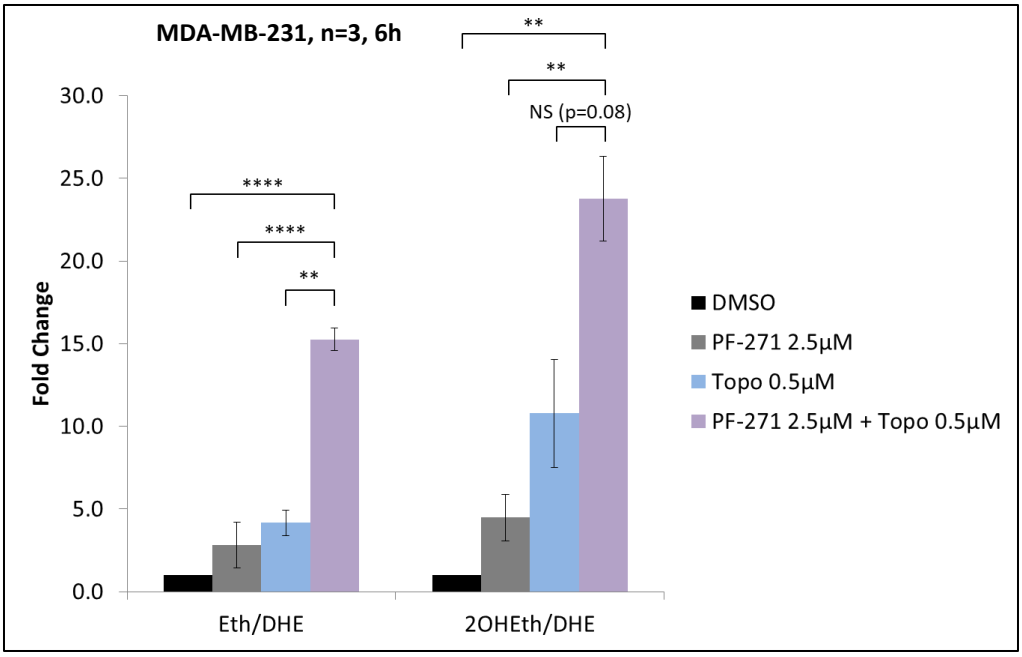

Figure 21: ROS accumulation in MDA-MB-231 following Combination PF-271/Topotecan Treatment

HPLC analysis of MDA-MB-231 cells following 6h treatment with PF-271 and topotecan. Ratios of ethidium : dihydroethidium (Eth/DHE) and 2-hydroxyethidium : dihydroethidium (2OHEth/DHE) are listed. Results shown are derived from an average of n=3, +/- SE.

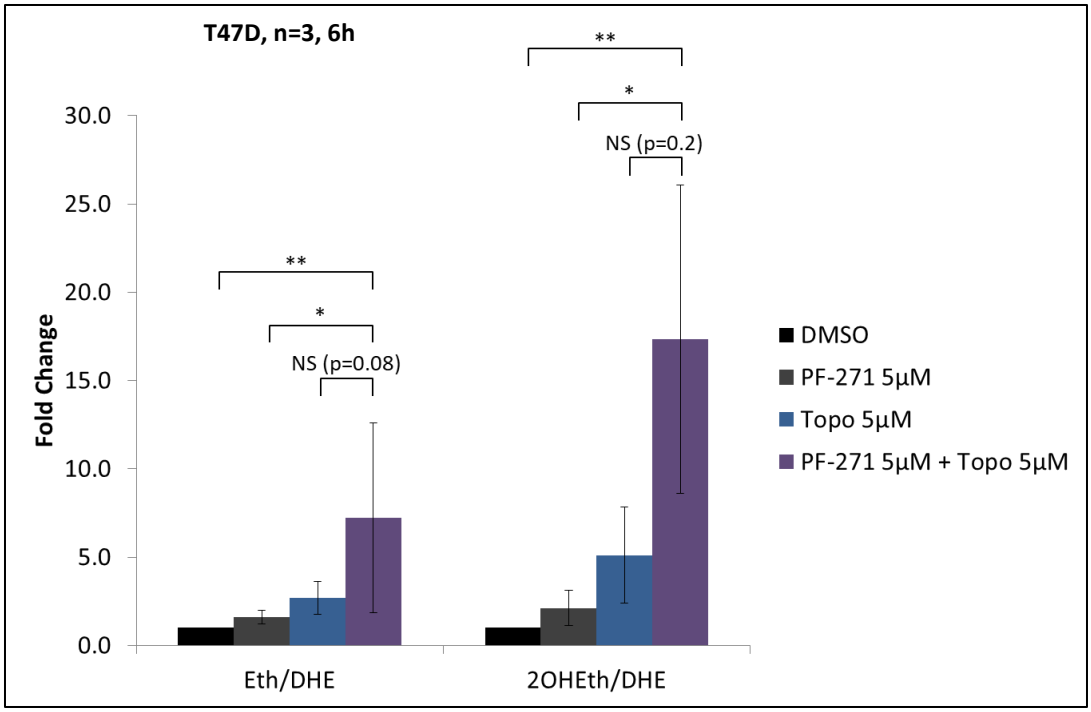

Figure 22: ROS accumulation in T47D following Combination PF-271/Topotecan Treatment

HPLC analysis of MDA-MB-231 cells following 6h treatment with PF-271 and topotecan. Ratios of ethidium : dihydroethidium (Eth/DHE) and 2-hydroxyethidium : dihydroethidium (2OHEth/DHE) are listed. Results shown are derived from an average of n=3, +/- SE.

Chapter 4: Discussion

Breast cancer claims thousands of lives every year. Metastatic breast cancer, like all metastatic diseases, is incurable and ultimately fatal. New treatment options are desperately needed for these women. The cytoplasmic tyrosine kinase FAK, a critical regulator and promoter of metastatic behavior and progression, has been shown to inversely affect survival. However, single-agent targeting of FAK has proved to be ineffective as a treatment option. In this study, therefore, we endeavoured to improve existing treatment regimens for metastatic breast cancer by combining a panel of standard of care chemotherapeutics with a small molecule FAK inhibitor with the hope of discovering a novel synergistic combination that decreases metastatic breast cancer viability.

In the study presented herein, my work has demonstrated the ability of a commercial FAK inhibitor, PF-271, to decrease both pY397 FAK levels and viability in metastatic breast cancer lines *in vitro*. After investigating numerous different classes of chemotherapeutics, those that promote DNA damage, specifically topoisomerase-inhibiting compounds, promotes a synergistic decrease in cell viability as measured by MTT at low concentrations of both PF-271 and topoisomerase inhibitor. This study also demonstrated that, while there is a decrease in cell viability when assessed via MTT assay, there is no decrease in cell number when detected via trypan blue assay, no increase in apoptotic cell death via flow cytometry, nor a decrease in survival signals via qRT-PCR. However, a distinct and potent increase in ROS was detected following treatment with both PF-271 and a model topoisomerase inhibitor in combination. This suggests that the effects on cell viability at 48h observed via MTT assay may be reflective of reduced cell metabolism or interference of the assay by ROS. There is also preliminary data suggesting that topoisomerase inhibitors induce FAK phosphorylation. In all, this study shows that with combining topoisomerase inhibitors with a FAK inhibitor induces a decrease in the viability in metastatic breast cancer cells, or minimally their metabolic activity, and promotes a significant increase in ROS, as well as possibly increasing FAK phosphorylation, all without inducing cell death or decreasing survival.

4.1 Regarding the Discrepancy between Cell Viability and Cell Death

The discrepancy that exists between the decreased cell viability results derived using MTT and the lack of cell death results indicated via flow cytometry and trypan blue exclusion assays merits note. MTT assays measure cell viability via the catalytic conversion of MTT into formazan via NAD(P)H-dependent oxidoreductase enzymes, and these enzymes are extremely sensitive to changes in metabolic activity (82). Therefore, a well-known limitation of MTT assays is the ability to accurately measure the impact of metabolic activity-altering compounds. It may give the impression of cell death, but it is in fact just a decrease in enzymatic activity.

This finding also corroborates with data suggesting an increased number of cells arrested at G2/M following treatment with PF-271 **(Figure 11)**. This effect is also visible in combination with topotecan, where the prominent G1/S arrest caused by topotecan is still apparent, and yet there is an identifiable G2/M arrest occurring as well. This could be interpreted as an additive effect, where cells which manage to escape the topotecan-induced G1/S arrest are later arrested at G2/M by PF-271. Still, there is no increase in apoptotic cell death when both compounds are used simultaneously. This could imply that these cells are experiencing a form of senescence. For example, following escape from G1/S arrest, cells that manage to also escape the PF-271-induced G2/M arrest enter senescence due to some combinatorial effect. These effects could be due to the increase in ROS produced by both compounds when used in combination, as such an increase would affect typical metabolic functioning, and possibly induce cell senescence (addressed below in Section 4.3). This theory could be further explored using senescence assays such as β-galactosidase, to observe if there is an increased in senesced cells following treatment with each drug in isolation compared to both drugs in combination.

However, this is not meant to imply that the data is not without merit. Despite not necessarily affecting cell apoptosis, synergistic inhibition of cell metabolism may yet still translate into important

clinical findings. Arrest of cell growth or inhibition of metabolism may even important implications, especially in a palliative context. In such a context, even if the tumour cells are still alive, a decrease in metabolic activity can lead to a meaningful increase in progression-free survival (83). Such conjecture would have to be confirmed *in vivo* first however. While the lack of cell death would likely mean that the PF-271/topotecan combination is unlikely to have an effect on overall survival rates, which may seem comparatively disappointing, it is crucial to remember that progression-free survival is correlated with lower morbidity and a higher quality of life (84). As such, tumour cells that experience a prolonged cell cycle arrest could translate into better progression-free survival for metastatic patients. Therefore, further investigations into these combination treatments in an *in vivo* setting for delays in metastatic tumour progression and growth.

4.2 Addressing Negative Combinations from Preliminary Panel

While it is important to focus on the positive results garnered from the topoisomerase inhibiting agents, it is equally important to speculate on the negative results produced from the other compounds tested in this study.

Firstly, it is important to address the lack of response produced by the hormone blocking agent anastrozole **(Figure 5, Panel A).** While exposure to anastrozole has been shown in the literature to produce a decrease in viability at 48h, the effect is very modest, less than 10% decrease compared to untreated cells in most cases, and typically shown only for cells that have been grown in hormone-free media (18). This is important as anastrazole functions as an aromatase inhibitor. As the name implies, aromatase inhibitors prevent the production of estrogen from androgens by inhibiting the enzyme aromatase. This mechanism of action would therefore have little to no effect on cells grown in hormone-containing media, as estrogen production via aromatase would be redundant. It is worth mentioning then, that all the cells used in this study were grown in media containing phenol-red, an

estrogenic compound, and FBS, which contains a variety of growth factors including estrogen. It should therefore come as no surprise that anastrazole failed to produce any indication of reduced cell viability as a single agent, nor when combined with PF-271. However, that is not to say that hormone blocking agents do not still have potential for synergy when used in combination with FAK inhibition. In particular, the use of an estrogen receptor blocking agent, such as tamoxifen, may produce different results, especially as FAK is known to crosstalk with a variety of growth receptors, including estrogen receptors (85). It could therefore be postulated that using a more direct hormone blocking compound such as tamoxifen in conjunction with a FAK inhibiting agent could decrease the proliferation rate of the cells. However, such conjecture is beyond the scope of this study, though it is very much deserving of investigation.

The antagonism of the microtubule inhibitors in response to the inclusion of PF-271 in the drug treatment was unexpected, and the mechanism behind this effect is unclear **(Figure 5, Panel B)**. A possible explanation lies in the size of the compounds. Vinorelbine (mw=778.932g/mol) and docetaxel (mw=807.879g/mol), are much larger molecules than the other chemotherapeutics investigated in this study (ex. cisplatin=300.01g/mol, doxorubicin=543.52g/mol, topotecan=457.9g/mol). Therefore, they rely more heavily on active transport methods to enter into the cell. Among others, the induction of P-glycoprotein mediated endocytosis is critical to the efficiency of vinorelbine, and docetaxel (86) (87). This appears to not be an obstacle to vinorelbine's efficacy at higher concentrations however, as shown by its ability in our study to effectively decrease cell viability at higher doses. However, modulation of endocytosis efficiency may affect the ability of the drug to cross into the cytoplasm at lower concentrations. This is shown by the fact that concomitant treatment of vinorelbine with other drugs that affect P-glycoprotein, a surface protein key to endocytosis of a variety of drugs, are known to modulate vinorelbine's efficacy (88). With this in mind, it is important to note that FAK is a known facilitator of active transport and endosome signalling in cells (89) (90). It follows that, potentially, while

high concentrations of a FAK inhibitor would produce decreased cell viability in isolation, low concentrations of a FAK inhibitor may simply decrease endosome signalling, limiting its impact on the cell. In fact, this has been shown to be the case in the literature, particularly in the case of large viral particles (91). Therefore, since vinorelbine is at least partially dependant on endocytosis formation and signalling in order to function, and inhibition of FAK impedes endosomal signalling, combining a vinorelbine-like agent with a FAK inhibitor would produce an antagonistic increase in cell viability when used in combination. While this is far from the only possible explanation, it merits further investigation.

Lastly, there is the initially implied, but ultimately fruitless, attempt to discern synergy between the generic non-topoisomerase inhibiting DNA damaging agents cisplatin, 5-fluorouacil and cyclophosphamide **(Figure 6 & Figure 8)** that must be addressed. Again, the mechanism of this specificity is unclear. It has been noted previously that a reduction in FAK activity sensitizes cells to the effects of non-specific DNA damage, including damage produced via ionizing radiation (63) (92). It is therefore unclear why the cross-linking effects of cisplatin or the anti-metabolite effects of 5-fluorouracil produced such underwhelming results. This could be due to a technical limitation regarding our ability to detect such a change, or may perhaps may require time points longer than 48h to observe the effects of these agents on cell viability. So while there is still the possibility that synergy, however slight, exists for these three compounds as well, it is beyond our ability to detect given the experimental methods used in this study.

Alternatively, the lack of response from generic DNA damaging agents may indeed imply a topoisomerase inhibitor-specific effect on cellular viability and metabolic activity. This would clearly be a novel finding as there is little evidence in the literature suggesting a specific link between FAK and topoisomerase activity at the time of writing. The only research that links the two is a paper detailing how the expression RNA topoisomerase Top3β is directly correlated with FAK expression levels (93).

Thus, we felt it was pertinent to pursue further investigation in order to elucidate the specifics mechanisms of such an interaction.

4.3 Proposed Mechanism of Action for Topoisomerase/FAK Inhibition

The data gathered within this study does provide us with some helpful clues to potentially develop a model for why such a complex relationship would exist between topoisomerase-inhibitors and FAK inhibitors. A critical clue lies in the fact that combining the two compounds does not result in an increased rate of cell death, via apoptosis or otherwise, but there is a clear and significant decrease in cell viability observed via MTT. This implies that the decrease in cell viability observed via MTT is due to a synergistic decrease in metabolic activity or due to cell cycle arrest.

Such a specific decrease in cell activity in the absence of cell death could be explained by the marked increase in ROS produced following treatment with both PF-271 and topotecan. While our experiments were unfortunately unsuccessful in replicating this effect in topotecan, an increase in toxic ROS following topoisomerase inhibition is an extremely well-documented phenomenon (81) (94). This is also known to be true of topotecan in MCF7 cells (95). Potential reasons for this lack of an effect could be as simple as the impact on ROS production following topotecan treatment in these cell lines may not be potent enough for us to identify it via HPLC; confounded by the necessary inclusion of DMSO in our treatments; or may be derived from the highly sensitive nature of HPLC providing too much variability for proper statistical assessments, among other possible complications.

Regardless, this well-known side effect is particularly important in this circumstance as ROS have been shown to directly induce double stranded breaks and inhibit topoisomerase functionality, thereby increasing the impact of treatment with compounds like topotecan (96). This is in addition to ROS's well-documented impact on NADPH-dependant enzymatic function, which would affect the readouts derived from MTT assays as mentioned earlier (82) (97). This produces a positive feedback loop where

topoisomerase inhibition leads to ROS production, which leads to further topoisomerase inhibition. This inevitably produces insurmountable levels of toxic ROS and DNA damage leading to decreased cell viability **(Figure 23)**.

Conversely, there is extensive documentation regarding FAK regulation via oxidative stress. Critically, that increased levels of ROS induce FAK expression and phosphorylation (98) (99) (100). This effect is implied in our preliminary data showing that treatment with topotecan, which is known to produce an increase in ROS levels, induces FAK phosphorylation **(Figure 16 & 17)**. This may prove to be a novel finding upon confirmation of the effect as, at the time of writing, there is no precedent for topoisomerase inhibition promoting FAK activity in the existing literature.

This could potentially be interpreted as a feedback loop, with high ROS promoting FAK activity and decreased FAK phosphorylation resulting in increased ROS accumulation. It could also be interpreted as a compensatory survival mechanism, however the lack of an increase in Bcl and Bcl2-L1, survival signals known to be affected by FAK expression (79) (80), places doubt in this theory **(Figure 18)**. However, there are a plethora of other survival signals modulated by FAK not covered by this study so far, including members of the JNK (38) and PI3K-Akt pathways (46) among others. So while there may be potential validity to this theory, it would require significant further investigation to prove conclusively.

Regardless, the disruption of this feedback loop could be the reason behind the large increases in ROS observed following combination treatment with topotecan and PF-271 **(Figures 20 - 22).** It would be reasonable to assume then, that, in the face of overwhelming oxidative stress and double stranded breaks that the cells would suffer from an inability to perform typical metabolic functions. While there is a need for low levels of ROS for typical progression of the tricarboxylic acid (TCA) cycle and the electron transport chain, excess ROS would induce a variety of toxic effects, as described previously (97). These toxic effects include mitochondrial DNA damage and inhibition of enzymes critical to the progression of

the TCA cycle, both of which can lead to cell death. All of these effects also affect MTT assay readouts, as described earlier (82) (97). However, a variety of malignant cancer subtypes are known to express higher ROS levels than their counterpart normal cells and have developed adaptive mutations to deal with this constantly elevated ROS levels (101). These adaptive mechanisms activate ROS scavenging proteins such as the superoxide dismutases SOD1, SOD2 and SOD3, as well as the inhibition of apoptotic pathways triggered by excess ROS (101).

It is also worth noting that the concentrations of PF-271 and topotecan identified as producing a spike in ROS are distinct from those identified as synergistically decreasing cell viability earlier via MTT. This could be due to a number of factors, but the most likely of which lies in the different treatment times between the two methods. The MTT readings were collected at 48h whereas the HPLC readings were acquired at 6h. These sensitivity differences may be due to cell line-specific differences in ROS pathway expression and efficacy. While it is yet unknown if this is the case, performing HPLC analysis again at later time points (such as 8h, 12h or 24h) may provide key details regarding ROS metabolism in these cells before the increased levels of apoptosis produced by PF-271 and topotecan begin to influence the accuracy of the HPLC readings.

Therefore, it would be reasonable to assume the following possible model: the breast cancer cells treated *in vitro* within the confines of this study underwent oxidative stress in the presence of both drugs. This oxidative stress was spurred by the treatment with topoisomerase inhibitors which generates ROS as a side effect of its mechanism of action, and by the decrease of pY397 FAK by PF-271, which alleviated an inhibiting factor controlling ROS accumulation. This oxidative stress induces synergistic deficiencies in metabolic functioning, but is not potent enough to induce synergistic cell death by 48h **(Figure 23)**.

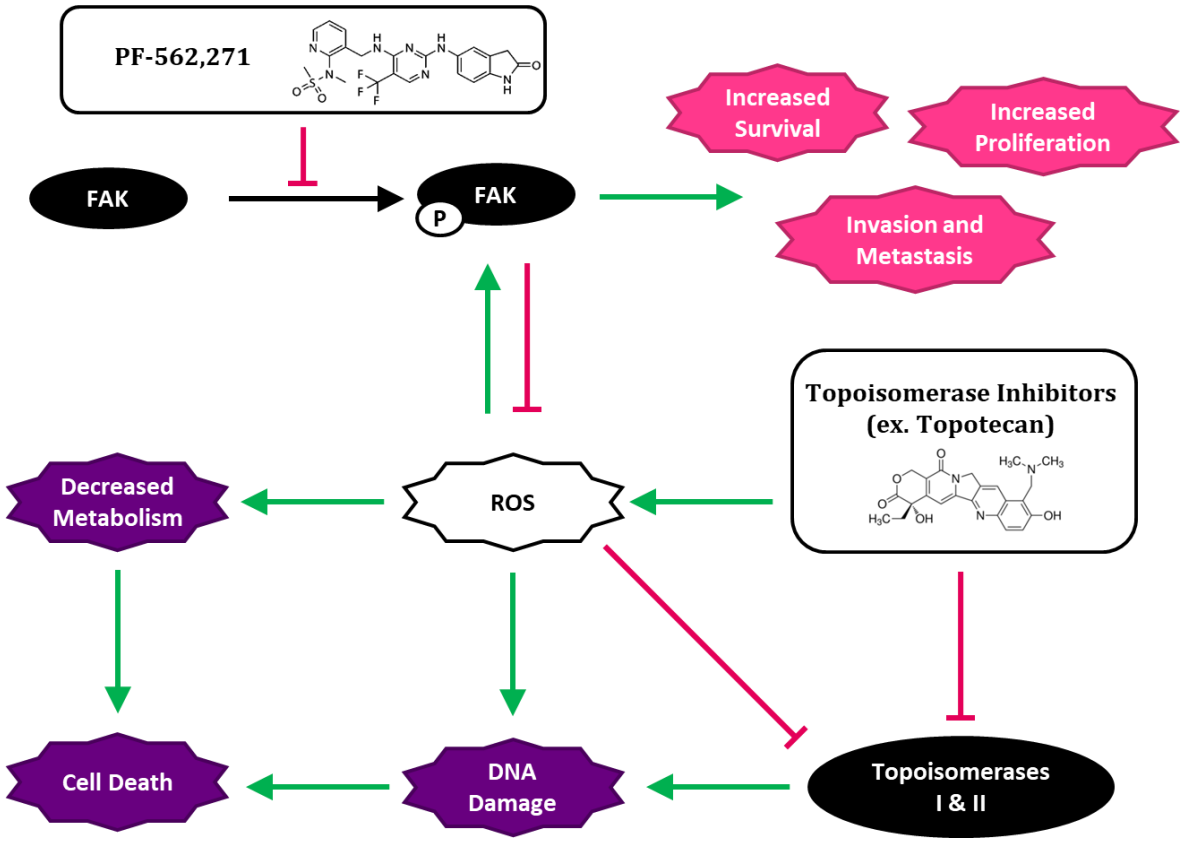

Figure 23: Overview of Proposed Mechanism of Action

Illustration of an overview of the proposed mechanism showing the interaction of topoisomerase inhibition and FAK inhibition. Special note should be made regarding the production of ROS by treatment with PF-562,271 and topoisomerase inhibition. Black arrows indicate phosphorylation, green arrows indicate upregulation, and red T-bars denote inhibitory regulation.

4.4 Conclusion & Future Directions

Firstly, further research should be performed to confirm some of the more preliminary results presented herein. Following completion of necessary replicates, further exploration into which ROS-influencing pathways are affected in the absence of pY397 FAK should be performed. Such investigations could include the expression levels of members of the superoxide dismutase family (ex. SOD1, SOD2 or SOD3) or 4-hydroxynonanol lipid peroxidation assays, to observe they are affected by FAK activity levels. One could also determine if ROS is critical to the decrease in cell viability observed by MTT by combining the topoisomerase inhibitors with PF-271 in the presence of an artificial ROS neutralizing agent such as N-acetyl-L-cysteine (NAC). Conversely, induction of ROS accumulation via chemical SOD inhibition or treatment with low doses of H_2O_2 could be performed to observe if the PF-271/topoisomerase inhibitor effect can be amplified in the presence of additional ROS. Lastly, in order to address the decrease in mitochondrial activity observed via MTT, additional investigations, including long chain qPCR assays for mitochondrial DNA damage known to be caused by ROS, or a SAβ-galactosidase assay in order to quantify the number of cells in senescence, could be performed.

Ultimately, while this study is forced to reject the hypothesis that combining a FAK inhibitor with current standard of care treatments for metastatic breast cancer would result in increased cell death and anti-tumour activity, it is not without its merits. If PF-271 is ever to be used as an effective cancer treatment, its biochemical pathways and influences on the effects on other drugs should be well examined. It can be heavily implied that PF-271, or any future FAK inhibitors, should not be used with drugs which are dependent on endosomal transport. It can also be stated that, while PF-271 combining with topoisomerase inhibitors did not produce synergistic cell death, the synergetic decrease in cell viability may yet have use in a progression-free palliative context. It is

also worth noting that the discovery of the pY397 FAK/ROS feedback loop is novel and may yet have implications beyond a cancer context. One could also take the results from this study as a suggestion to support research into compounds which promote ROS generation beyond what PF-271 is capable of in combination with topoisomerase inhibitors.

Bibliography

1. **Canadian Cancer Society's Advisory Committee on Cancer Statistics.** *Canadian Cancer Statistics 2015.* Toronto, ON : Canadian Cancer Society, 2015.

2. **Howlader N, Noone AM, Krapcho M, Miller D, Bishop K, Altekruse SF, Kosary CL, Yu M, Ruhl J, Tatalovich Z, Mariotto A, Lewis DR, Chen HS, Feuer EJ, Cronin KA.** *SEER Cancer Statistics Review.* Bethesda, MD : National Cancer Institute, 1975-2013. Based on November 2015 SEER data submission, posted to the SEER web site, April 2016.

3. **Cancer Research UK.** *Breast Cancer Survival Statistics.* London, UK : Cancer Research UK, 2017.

4. **Kreipe H, Sinn HP.** A Brief Overview of the WHO Classification of Breast Tumors, 4th Edition, Focusing on Issues and Updates from the 3rd Edition. *Breast Care (Basel).* April 26, 2013, Vol. 8, 2, pp. 149-154.

5. **Malhottra GK, Zhao X, Band H, Band V.** Histological, molecular and functional subtypes of breast cancers. *Cancer Biology Therapy.* November 15, 2010, Vol. 10, 10, pp. 955-960.

6. **American Cancer Society.** *Cancer Facts & Figures 2015 (includes the Special Section: Breast Cancer In Situ).* Atlanta, GA : American Cancer Society, 2015.

7. **Leste SC, et al.** Protocol for the examination of specimens from patients with invasive carcinoma of the breast. *Archives of Pathology & Laboratory Medicine.* October 2009, Vol. 133, 10, pp. 1515-1538.

8. **BreastCancer.org.** Molecular Subtypes of Breast Cancer. [Online] November 9, 2016. [Cited: 12 2017, August.] http://www.breastcancer.org/symptoms/types/molecular-subtypes.

9. **Xiaofeng D, et al.** Breast cancer intrinsic subtype classification, clinical use and future trends. *American Journal of Cancer Research.* September 15, 2015, Vol. 5, 10, pp. 299-2943.

10. **Ribelles N, et al.** Pattern of recurrence of early breast cancer is different according to intrinsic subtype and proliferation index. *Breast Cancer Research.* October 22, 2013, Vol. 15, 5, p. R98.

11. **Kumar N, et al.** Prevalence of molecular subtypes of invasive breast cancer: A retrospective study. *Medical Journal Armed Forced India.* July 2015, Vol. 71, 3, pp. 254-258.

12. *Detailed Guide: Bone Metastasis.* **American Cancer Society.** Atlanta : American Cancer Society, 2009.

13. **Allan L, et al.** Randomized Active-Controlled Phase II Study of Denosumab Efficacy and Safety in Patients With Breast Cancer-Related Bone Metastases. *Journal of Clinical Oncology.* October 1, 2007, Vol. 25, 28.

14. **Braun S, et al.** A Pooled Analysis of Bone Marrow Micrometastasis in Breast Cancer. *New England Journal of Medicine.* August 25, 2005, 353, pp. 793-802.

15. **Longley DB, Harkn DP, Johnston PG.** 5-Fluorouracil: mechanisms of action and clinical strategies. *Nature Reviews Cancer.* 2003, 3, pp. 330-338.

16. **National Comprehensive Cancer Network.** http://www.nccn.org/professionals/physician_gls/f_guidelines.asp. *NCCN Clinical Practice Guidelines in Oncology: Breast Cancer (Version 2.2015).* [Online] National Comprehensive Cancer Network, February 2015.

17. **National Cancer Insitute.** *Breast Cancer Treatment for Health Professionals (PDQ®).* s.l. : National Cancer Insitute, 2015.

18. **Xanathopoulos JM, Romano AE, Kajumdar SK.** Response of Mouse Breast Cancer Cells to Anastrozole, Tamoxifen, and the Combination. *Journal of Biomedicine and Biotechnology.* 2005, Vol. 205, 1, pp. 10-19.

19. **Maximiano S, Magalhães P, Guerreiro MP, Morgado M.** Trastuzumab in the Treatment of Breast Cancer. *BioDrugs.* April 30, 2016, Vol. 30, 2, pp. 75-86.

20. **Coleman RE, McCloskey EV.** Bisphosphonates in oncology. *Bone.* July 2011, Vol. 49, 1, pp. 71-76.

21. **Zhu X, Verma S.** Targeted therapy in HER2-positive metastatic breast cancer: a review of the literature. *Current Oncology.* March 2015, Vol. 22, S1, pp. S19-S28.

22. **Van Poznak C, et al.** Use of biomarkers to guide decisions on systemic therapy for women with metastatic breast cancer: American Society of Clinical Oncology clinical practice guideline. *Journal of Clinical Oncology.* August 2015, Vol. 34, 24, pp. 2695-2706.

23. **Thompson WR, Rubin CT, Rubin J.** Mechanical regulation of signaling pathways in bone. *Gene.* July 25, 2012, Vol. 503, 2, pp. 179-193.

24. **Gözde G, et al.** A comprehensive review of denosumab for bone metastasis in patients with solid tumors. *Current Medical Research and Opinion.* 2016, Vol. 32, 1, pp. 135-145.

25. **S, Dawood and al, et.** Trends in Survival Over the Past Two Decades Among White and Black Patients With Newly Diagnosed Stage IV Breast Cancer. *Journal of Clinical Oncology.* October 20, 2008, Vol. 26, 30.

26. **Weide R, et al.** Metastatic breast cancer: prolongation of survival in routine care is restricted to hormone-receptor- and Her2-positive tumors. *SpringerPlus.* September 17, 2014, 3, p. 535.

27. **Masuda H, et al.** Role of Epidermal Growth Factor Receptor in Breast Cancer. *Breast Cancer Research and Treatment.* November 18, 2013, Vol. 136, 2, pp. 331-345.

28. **Sainsbury JR, Farndon JR, Needham GK, Malcolm AJ, Harris AL.** Epidermal-growth-factor receptor status as predictor of early recurrence of and death from breast cancer. *Lancet.* June 20, 1987, Vol. 329, 8547, pp. 1398-1403.

29. **Lu Z, Jiang G, Blume-Jensen P, Hunter T.** Epidermal Growth Factor-Induced Tumor Cell Invasion and Metastasis Initiated by Dephosphorylation and Downregulation of Focal Adhesion Kinase. *American Society for Microbiology: Molecular and Cellular Biology.* 2001, Vol. 21, 12, pp. 4016-4031.

30. **Howe G, et al.** Focal Adhesion Kinase Inhibitors in Combination with Erlotinib Demonstrate Enhanced Anti-Tumor Activity in Non-Small Cell Lung Cancer. *PLOS One.* 2016, Vol. 11, 3, p. e0150567.

31. **Uhlén M, et al.** Tissue-based map of the human proteome. *Science.* 2015, Vol. 247, 6220, p. 1260419.

32. **Mitra SK, Hanson DA, Schlaepfer DD.** Focal Adhesion Kinase: In Command and Control of Cell Motility. *Nature Reviews Molecular Cell Biology.* 6, January 2005, pp. 56-68.

33. **Zhao, X and Guan, JL.** Focal adhesion kinase and its signaling pathways in cell migration and angiogenesis. *Advanced Drug Delivery Reviews.* July 18, 2011, pp. 610-615.

34. **Frame MC, et al.** The FERM domain: organizing the structure and function of FAK. *Nature Reviews Molecular Cell Biology.* 11, 2011, pp. 802-814.

35. **Plow E, et al.** Ligand Binding to Integrins. *Journal of Biological Chemistry.* May 4, 2000, 275, pp. 21785-21788.

36. **Iskratsch T, Wolfenson H, Sheetz MP,.** Appreciating force and shape — the rise of mechanotransduction in cell biology. *Nature Reviews Molecular Cell Biology.* October 14, 2014, 15, pp. 825-833.

37. **Leitha D, et al.** Structural basis for the autoinhibition of focal adhesion kinase. *Cell.* 2007, 129, pp. 1177-1187.

38. **Sulzmaier FJ, Christine J, Schlaepfer DD.** FAK in Cancer: Mechanistic Findings and Clinical Applications. *Nature.* 14, August 07, 2014, pp. 598-610.

39. **Fan H, Guan JL.** Compensatory function of Pyk2 protein in promotion of focal adhesion kinase (FAK)-null mammary cancer stem cell tumorigenicity and metastatic activity. *Journal of Biological Chemistry.* 286, pp. 18573-18582.

40. **Lim ST, et al.** Pyk2 inhibition of p53 as an adaptive. *Journal of Biological Chemistry.* 2010, 285, pp. 1743-1753.

41. **Lim Y, et al.** Pyk2 and FAK connections to p190Rho guanine nucleotide exhange factor regulare RhoA activity, focal adhesion formation, and cell motility. *Journal of Cell Biology.* 2008, Vol. 180, pp. 187-203.

42. **Weis SM, et al.** Compensatory role for Pyk2 during angiogenesis in adult mice lacking endothelial cell FAK. *Journal of Cell Biology.* 2008, Vol. 181, pp. 43-50.

43. **Hanahan D, Weinberg R.** Hallmarks of Cancer: The Next Generation. *Cell.* March 4, 2011, Vol. 144, 5, pp. 646-647.

44. **Zhao, J-H, Reiske, Heinz and J-L, Guan.** Regulation of the Cell Cycle by Focal Adhesion Kinase. *Journal of Cell Biology.* 1998, Vol. 143, 7, pp. 1997-2008.

45. **Shibue T, Weinberg R.** Integrin β1-focal adhesion kinase signaling directs the proliferation of metastatic cancer cells disseminated in the lungs. *PNAS.* 2009, Vol. 106, 25, pp. 10290-10295.

46. **Zhao J, Guan JL.** Signal transduction by focal adhesion kinase in cancer. *Cancer Metastasis Review.* 2009, 28, pp. 35-49.

47. **Manning B, Cantley L.** AKT/PKB Signaling: Navigating Downstream. *Cell.* June 29, 2007, Vol. 129, 7, pp. 1261-1274.

48. **Golubovskaya VM, Cance W.** FAK and p53 Protein Interactions. *Anti-cancer Agents in Medicial Chemistry.* 2011, Vol. 11, 7, pp. 617-619.

49. **Ozaki T, Nakagawara A.** Role of p53 in Cell Death and Human Cancers. *Cancers (Basel).* March 2011, Vol. 3, 1, pp. 994-1013.

50. **Uruno T, et al.** Activation of Arp2/3 complex-mediated actin polymerization by cortactin. *Nature Cell Biology.* 2001, 3, pp. 259-266.

51. **Provenzano PP, Inman DR, Eliceiri KW, Keely PJ.** Mammary epithelial-specific disruption of focal adhesion kinase retards tumor formation and metastasis in a transgenic mouse model of human breast cancer. *American Journal of Pathology.* November 2008, Vol. 173, 5, pp. 1551-15565.

52. **The Cancer Genome Atlas Network.** Comprehensive Molecular Portraits of Human Breast Tumours. *Nature.* 490, October 4, 2012, pp. 61-70.

53. **Golubovskaya VM.** Focal Adhesion Kinase as a Cancer Therapy Target. *Anti-Cancer Agents in Medicinal Chemistry.* 2010, Vol. 10, 10, pp. 735-741.

54. **McLean GW, et al.** The Role of Focal Adhesion Kinase in Cancer - A New Therapeutic Opportunity. *Nature Reviews Cancer.* 5, July 2005, pp. 505-515.

55. **Kurio N, et al.** Anti-tumor effect in human breast cancer by TAE226, a dual inhibitor for FAK and IGF-IR in vitro and in vivo. *Experimental Cell Research.* 2011, 317.

56. **Stokes JB, et al.** Inhibition of focal adhesion kinase by PF-562,271 inhibits the growth and metastasis of pancreatic cancer concomitant with altering the tumor microenvironment. *Molecular Cancer Therapeutics.* November 2011, Vol. 10, 11, pp. 2135-2145.

57. **Lee BY, Timpson P, Horvath L, Daly RJ.** FAK signaling in human cancer as a target for therapeutics. *Pharmacology & Therapeutics.* February 2015, Vol. 146, pp. 132-149.

58. **Arora A, Scholar EM.** Role of Tyrosine Kinase Inhibitors in Cancer Therapy. *Journal of Pharmacolpgy and Experimental Therapeutics.* 215, December 2005, Vol. 3, pp. 971-979.

59. **Pan G, Ke S, Zhao J.** Comparison of the efficacy and safety of single-agent erlotinib and doublet molecular targeted agents based on erlotinib in advanced non-small cell lung cancer (NSCLC): a systematic review and meta-analysis. *Targeted Oncology.* 2013, Vol. 8, 2, pp. 107-116.

60. **National Comprehensive Cancer Network (NCCN).** Practice Guidelines in Oncology: Breast Cancer. Version 2.2017. [Online] [Cited: August 28, 2017.] www.nccn.org.

61. **Schott, AF.** Systemic treatment for HER2-positive metastatic breast cancer. [Online] [Cited: August 28, 2017.] https://www.uptodate.com/contents/systemic-treatment-for-her2-positive-metastatic-breast-cancer?source=search_result&search=breast%20cancer%20treatment&selectedTitle=16~150.

62. **Jyotsnabaran H, et al.** Focal Adhesion Kinase Silencing Augments Docetaxel-Mediated Apoptosis in Ovarian Cancer Cells. *Clinical Cancer Research.* December 15, 2005, Vol. 11, 24, pp. 8829-8836.

63. **Tavora B, et al.** Endothelial-cell FAK targeting sensitizes tumours to DNA-damaging therapy. *Nature.* 514, October 2, 2014, pp. 112-116.

64. **Lazaro G, et al.** Targeting Focal Adhesion Kinase in ER+/HER+ breast cancer improves trastuzumab response. *Endocrine-Related Cancer.* 20, October 1, 2013, pp. 691-704.

65. **Lacroix M, Leclercq G.** Relevance of Breast Cancer Cell Lines as Models for Breast Tumours: An Update. *Breast Cancer Research and Treatment.* February 2004, Vol. 83, 3, pp. 249-289.

66. **Wasielewski M, Elstrodt F, Klijn JG, Berns EM, Schutte M.** Thirteen new p53 gene mutants identified among 41 human breast cancer cell lines. *Breast Cancer Research and Treatment.* September 2006, Vol. 99, 1, pp. 97-101.

67. **Nigro JM, et al.** Mutations In The P53 Gene Occur In Diverse Human-tumor Types. *Nature.* 1989, Vol. 342, 6250, pp. 705-708.

68. **Bartek J, Iggo R, Gannon J, Lane DP.** Genetic and immunochemical analysis of mutant p53 in human breast cancer cell lines. *Ongogene.* 1990, Vol. 5, 6, pp. 893-899.

69. **Holliday DL, Speirs V.** Choosing the right cell line for breast cancer research. *Breast Cancer Research.* August 12, 2011, Vol. 13, 4, p. 215.

70. **Burger D, et al.** Endothelial Microparticle Formation by Angiotensin II Is Mediated via Ang II Receptor Type I/NADPH Oxidase/ Rho Kinase Pathways Targeted to Lipid Rafts. *Arteriosclerosis, Thrombosis, and Vascular Biology.* July 20, 2010, Vol. 2011, 31, pp. 1898-1907.

71. **Miller WR.** Aromatase inhibitors: mechanism of action and role in the treatment of breast cancer. *Seminars in Oncology.* August 2003, Vol. 30, 14, pp. 3-11.

72. **Ngan V, Bellman K, Hill B, Wilson L, Jordan MA.** Mechanism of Mitotic Block and Inhibition of Cell Proliferation by the Semisynthetic Vinca Alkaloids Vinorelbine and Its Newer Derivative Vinflunine. *Molecular Pharmacology.* July 2001, Vol. 60, 1, pp. 225-323.

73. **Yang F, Teves S, Kemp CJ, Henikoff S.** Doxorubicin, DNA torsion, and chromatin dynamics. *Biochimica et Biophysica Acta (BBA) - Reviews on Cancer.* January 2014, Vol. 1845, 1, pp. 84-89.

74. **Dasari S, Tchounwou PB.** Cisplatin in cancer therapy: Molecular mechanisms of action. *European Journal of Pharmacology.* October 2014, Vol. 740, pp. 364-378.

75. **Montecucco A, Zanetta F, Biamonto G.** Molecular mechanisms of etoposide. *EXCLI Journal.* 2015, 14, pp. 95-108.

76. **Rasheed Z, Rubin E.** Mechanisms of resistance to topoisomerase I-targeting drugs. *Oncogene.* 2003, 22, pp. 7296-7304.

77. **El-Serafi I, et al.** The mechanism of action of cyclophosphamide on the nephritis of (NZB x NZW)F1 hybrid mice. *PLOS One.* January 22, 2014, Vol. 9, 1, p. e86619.

78. **Berridge MV, Herst PM, Tan AS.** Tetrazolium dyes as tools in cell biology: new insights into their cellular reduction. *Biotechnology Annual Review.* 2005, 11, pp. 127-52.

79. **Sorenson CM, Sheibani N.** Focal adhesion kinase, paxillin, and Bcl-2: Analysis of expression, phosphorylation, and association during morphogenesis. *Developmental Dynamics.* August 1999, Vol. 215, 4, pp. 371-382.

80. **Yoon H, et al.** Targeted Inhibition of FAK, PYK2 and BCL-XL Synergistically Enhances Apoptosis in Ovarian Clear Cell Carcinoma Cell Lines. *PLOS One.* February 11, 2014, Vol. 9, 2, p. e88587.

81. **Wu SY, et al.** NPRL-Z-1, as a new topoisomerase II poison, induces cell apoptosis and ROS generation in human renal carcinoma cells. *PLoS One.* November 2014, Vol. 9, 11, p. e112220.

82. **Mosmann T.** Rapid colorimetric assay for cellular growth and survival: Application to proliferation and cytotoxicity assays. *Journal of Immunological Methods.* December 1983, Vol. 65, 1-2, pp. 55-63.

83. **Silva AS, Kam Y, Khin ZP, Minton SE, Gillies RJ, Gatenby RA.** Evolutionary Approaches to Prolong Progression-Free Survival in Breast Cancer. *Cancer Research.* 2012, Vol. 72, 24, pp. 6362-6370.

84. **Gutman SI, Piper M, Grant MD, et al.** Progression-Free Survival: What Does It Mean for Psychological Well-Being or Quality of Life? Rockville : Agency for Healthcare Research and Quality (US), 2013.

85. **Chang YL, et al.** Regulation of estrogen receptor α function in oral squamous cell carcinoma cells by FAK signaling. *Society for Endocrinology.* August 1, 2014, 21, pp. 555-565.

86. **Lagas JS, et al.** P-Glycoprotein, Multidrug-Resistance Associated Protein 2, Cyp3a, and Carboxylesterase Affect the Oral Availability and Metabolism of Vinorelbine. *Molecular Pharmacology.* October 2012, Vol. 82, 4, pp. 636-644.

87. **Miettinen S, Grènman S, Ylikomi T.** Inhibition of P-glycoprotein-mediated docetaxel efflux sensitizes ovarian cancer cells to concomitant docetaxel and SN-38 exposure. *Anti-Cancer Drugs.* April 2009, Vol. 20, 4, pp. 267-276.

88. **medac.** Vinorelbine 10 mg/ml Concentrate for solution for infusion- Summary of Product Characteristics (SPC) - (eMC). [Online] 2017. [Cited: September 18, 2017.] https://www.medicines.org.uk/emc/medicine/19453.

89. **Alanko J, Ivaska J.** Endosomes: Emerging Platforms for Integrin-Mediated FAK Signalling. *Trends in Cell Biology.* JUne 2016, Vol. 26, 6, pp. 391-398.

90. **Alanko J, et al.** Integrin endosomal signalling suppresses anoikis. *Nature Cell Biology.* 2015, 17, pp. 1412-1421.

91. **Elbahesh H, et al.** Novel Roles of Focal Adhesion Kinase in Cytoplasmic Entry and Replication of Influenza A Viruses. *Journal of Virology.* 2014, Vol. 88, 12, pp. 6714-6728.

92. **Tang KJ.** Focal Adhesion Kinase Regulates the DNA Damage Response and Its Inhibition Radiosensitizes Mutant KRAS Lung Cancer. *Clinical Cancer Research.* December 2016, Vol. 22, 23, pp. 5851-5863.

93. **Xu D, et al.** Top3β is an RNA topoisomerase that works with fragile X syndrome protein to promote synapse formation. *Nature Neuroscience.* September 2013, Vol. 16, 9, pp. 1238-1247.

94. **Banerji S, Los M.** Important Differences Between Topoisomerase-I and -II Targeting. *Cancer Biology & Therapy.* 2006, Vol. 5, 8, pp. 965-966.

95. **Timur M, Akbas SH, Ozben T.** The effect of Topotecan on oxidative stress in MCF-7 human breast cancer cell line. *Acta Biochimica Polonica.* 2005, Vol. 52, 4, pp. 897-902.

96. **Lu HR, et al.** Reactive oxygen species elicit apoptosis by concurrently disrupting topoisomerase II and DNA-dependent protein kinase. *Molecular Pharmacology.* October 2005, Vol. 68, 4, pp. 983-994.

97. **Wellen KE, Thompson CB.** Cellular metabolic stress: Considering how cells respond to nutrient excess. *Molecular Cell.* October 22, 2010, Vol. 40, 2, pp. 323-332.

98. **Ben Mahdi MH, Andrieu V, Pasquier C.** Focal adhesion kinase regulation by oxidative stress in different cell types. *IUBMB Life.* October-November 2000, Vol. 50, 4-5, pp. 291-299.

99. **Chiarugi P, et al.** Reactive oxygen species as essential mediators of cell adhesion. *Journal of Cell Biology.* June 9, 2003, Vol. 161, 5, pp. 933-944.

100. **Ribeiro-Pereira E, et al.** Redox Modulation of FAK Controls Melanoma Survival - Role of NOX4. *PLoS One.* June 7, 2014, Vol. 9, 6, p. e99481.

101. **Trachootham D, Alexandre J, Huang P.** Targeting cancer cells by ROS-mediated mechanisms: a radical therapeutic approach? *Nature Reviews Drug Discovery.* July 2009, 8, pp. 579-591.

Contributions of Collaborators

Preliminary western analysis and treatment of cells used for **Figure 16** and **Figure 17** was performed by Viya Vijithakumar, of the Addison Lab. Also, as described in Section 2.7, final HPLC analysis following pellet isolation was performed by Dr. Chet E Holterman, of the Dr. Chris Kennedy Lab at the Kidney Research Centre of the Ottawa Hospital.

Appendix

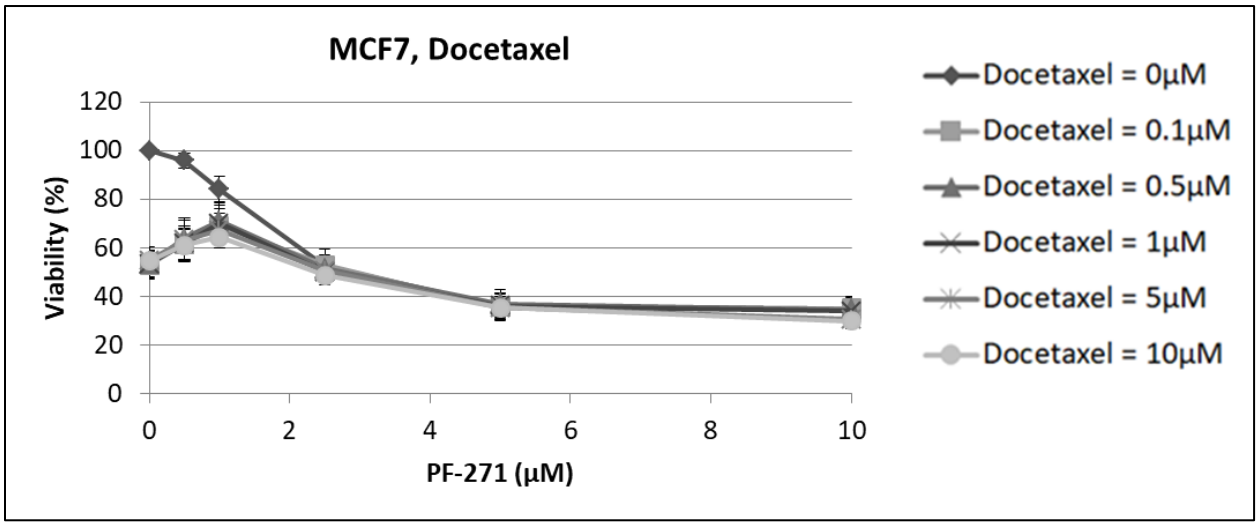

Supplementary Data 1: Combinations of PF-271 with Docetaxel in MCF7

MCF7 cells treated simultaneously with a gradient of PF-271, and 5-fluorouracil for 48h. Viability was measured using MTT, using DMSO as a vehicle control representing 100% viability. Shown are averages of n=3 biological replicates, +/-SE.